R. & M. No. 3510

MINISTRY OF TECHNOLOGY

AERONAUTICAL RESEARCH COUNCIL
REPORTS AND MEMORANDA

Examples of the Effects of Shock-Induced Boundary-Layer Separation in Transonic Flight

By H. H. Pearcey, B.Sc., and D. W. Holder, Ph.D.

LONDON: HER MAJESTY'S STATIONERY OFFICE
1967
PRICE £1 5*s*. 0*d*. NET

Examples of the Effects of Shock-Induced Boundary-Layer Separation in Transonic Flight

By H. H. Pearcey, B.Sc., and D. W. Holder, Ph.D.

Reports and Memoranda No. 3510*
January, 1954

Summary.

The present state of knowledge concerning the interaction between shock waves and boundary layers, and several examples of the importance of the interaction in high-speed flight were described in a previous report[1]. It was shown that the major effects arose from, and could be explained in terms of, separation of the boundary layer at or ahead of the shock wave. The present note gives further examples of the consequences in flight of shock-induced separation of the boundary layer; these examples have been derived from data obtained in NACA and British flight tests, and from high-speed wind tunnel experiments.

The variation of the pressure coefficient at the trailing edge of the wing has been used to deduce the onset of separation from the results of the flight tests. It is found that separation occurs on straight wings at approximately the same value of the local Mach number just ahead of the shock as for two-dimensional aerofoils with turbulent boundary layers. For swept wings the available data are inadequate for a detailed comparison. Various features in the "steady-flow" characteristics and buffeting behaviour of the aircraft considered are then shown to be closely associated with boundary-layer separation. These features include wing dropping, loss of control effectiveness, and the "pitch-up" instability which has been encountered with swept-back wings.

In an attempt to obtain a clearer understanding of the mechanism which leads to high-speed buffeting, a review is given of NACA wind-tunnel measurements of the pressure fluctuations at the surfaces of aerofoils and in their wakes. These observations show that large fluctuations may occur under the conditions for which separation would be expected; a detailed correlation with the onset of separation is not possible, however, because the data required are not available.

The effects of shock-induced separation are almost always undesirable, and several possible means for eliminating separation or for reducing its effects on current aircraft are, therefore, described. A scheme which has received much attention in recent investigations is the use of vortex generators; promising results have already been obtained, and it is thought that further improvements may be possible by the use of improved design. Other devices mentioned here include the use of fences, and boundary-layer control by suction and blowing.

It is suggested that at low incidences it should be possible to design the section and planform so that shock-induced separation is either absent or has negligible effects. Separation may still occur, however, for large incidences and control deflections, and interest will probably continue in the devices mentioned above.

---

*Replaces A.R.C. 16 446.

(Note added in 1967)

This Report could not be considered for publication when it was first issued because much of the information pertaining to specific aircraft was then classified. Although the subject has been developed very considerably in the intervening years, the original analysis and discussion are considered to be of sufficient historical interest and permanent value to merit publication in this, their original form.

LIST OF CONTENTS

1. *Introduction.*

The results of such flight tests as could be referred to in Ref. 1 indicated that conditions for the occurrence of shock-induced turbulent boundary-layer separation were very much the same as those observed in wind tunnel tests. It was suggested that the occurrence of buffeting could be correlated with and explained by the occurrence of separation and that many other undesirable phenomena encountered in transonic flight could be traced to the effects of the separation on the 'steady-flow' characteristics of wings and aerofoils. We now present certain further results which confirm and extend these findings.

The occurrence of separation can be derived from the extensive pressure plotting data now available for NACA research aeroplanes and certain effects observed on the same aeroplanes can be attributed directly to the separation. A limited amount of evidence on the occurrence of turbulent separation on swept wings is also available. The recent American work on buffet boundaries and pressure fluctuations can now be treated more fully. This applies also to investigations in the U.S.A. and this country of vortex generators as a remedy for separation; here again NACA flight tests have given valuable evidence on the effects of separation because they demonstrate which characteristics of the aeroplanes are improved when it is eliminated or reduced in extent.

In this Report we first give examples in which it is possible to determine from the available data the conditions under which shock-induced separation of the turbulent boundary layer occurs on wings, and then consider the correlation between these conditions and various characteristics of the wings both in steady flow and when buffeting occurs.

2. *Examples of the Occurrence of Shock-induced Turbulent Boundary-layer Separation on Aircraft Wings.*

Reference is made to the examples listed in Table I for which the occurrence of separation has been reported or can be deduced with confidence from other recorded data.

TABLE I

Examples of Shock-induced Turbulent Separation.

Aircraft	Section thickness (streamwise)	Wing sweep ($\frac{1}{4}$ chord)	Type of experiment	Method of observing or deducing the presence of separation	References
X–1–1 (XS–1)	8%	Nil	NACA flight pressure plotting	Divergence of $C_{pT.E.}$	2
X–1–2	10%	Nil	NACA flight pressure plotting	Divergence of $C_{pT.E.}$	3,4,5,6
D–558–I	10%	Nil	NACA flight pressure plotting	Divergence of $C_{pT.E.}$	7,8,9
Hawker P.1052	10% (thickened over the intakes)	35°	R.A.E. tunnel pressure plotting on half wing	Divergence of $C_{pT.E.}$	10
Valiant and Type 1000	9% (13% over the intakes)	approx. 30°	Vickers Armstrongs tunnel tests on half wings	Movement of oil and tufts	
Sabre (F–86A)	10%	35°	NACA flight tests with vortex generators	Inferred from positive effects of vortex generators	11

Table 1 continued on next page

TABLE I —*continued*

Examples of Shock-induced Turbulent Separation.

Aircraft	Section thickness (streamwise)	Wing sweep ($\frac{1}{4}$ chord)	Type of experiment	Method of observing or deducing the presence of separation	References
F–51D	16%	Nil	NACA flight tests with vortex generators	Inferred from positive effects of vortex generators plus boundary-layer traverses	12
—	12%	35°	NACA tunnel tests on half-wing	Changes in $\partial C_L/\partial\alpha$ and $\partial C_m/\partial C_L$	13

2.1. *NACA Flight Pressure-plotting Tests.*

The sketches of the X–1–1, X–1–2, and D–558–I wings in Fig. 1 show the spanwise stations appropriate to the pressure distributions used in the present report. The X–1–1 and X–1–2 have the same planform but the spanwise stations are different. The wing section shapes are the same, the thicknesses being 8 per cent and 10 per cent respectively. The D-558-I wing section is the same in thickness and shape as that of the X-1-2.

Results are available both for increasing Mach number at nearly constant normal-force coefficient (about 0·3 in each case), obtained either in level flight or in shallow dives, and for increasing normal-force coefficient at several nearly constant Mach numbers, obtained in pull-ups and 'wind-up' turns.

The occurrence of shock-induced separation in the runs for increasing Mach number can be deduced from the surface pressure measurements in much the same way as was found to apply for two-dimensional aerofoils when Mach number is increased at constant incidence, in Ref. 1. In particular, $C_{pT.E.}$, the pressure coefficient measured at the trailing-edge position, diverges from its smooth variation because the pressure recovery over the rear of the aerofoil is reduced by the separation and becomes progressively less complete as the Mach number is raised; it was shown in Ref. 1 that the point of divergence corresponds closely to the first occurence of separation.The rate at which the upper-surface shock* moves rearwards with increasing Mach number also undergoes a marked change when separation occurs. In many instances the movement is stopped[1] (or even reversed if the results are plotted for constant C_L).

These effects are shown clearly for the X-1-1 and D-558-I aircraft in Figs. 3 and 5 respectively in which $C_{pT.E.}$ and the chordwise position** of the shock are plotted against free-stream Mach number, M_0. The local Mach number,** M_1, just upstream of the shock on the upper surface is also plotted. For the X–1–1, Fig. 3, the divergence of $C_{pT.E.}$ and that in shock movement both occur at about the same free-stream Mach number, 0·815, and the local Mach number reached at this point is almost exactly the value for which separation was observed to occur in wind-tunnel tests on aerofoils[1] (shown by the dotted line crossing the curve of M_1***). The agreement is also fairly good for the D–558–I (Fig. 5); the local Mach number reaches 1·235, (the value observed for separation on aerofoils) when $M_0 = 0{\cdot}825$, whereas the divergence of $C_{pT.E.}$ and in shock movement occur when the local Mach number is 1·27, at $M_0 = 0{\cdot}84$.

For the X–1–2 aircraft, Fig. 4, separation was evidently present from the lowest speed of the run because $C_{pT.E.}$ was already falling and the upper-surface shock moving forwards. The local Mach number already exceeded that given by the empirical criterion for separation on aerofoils.

*i.e. the shock which first causes separation for an aerofoil or wing producing positive lift.

**The chordwise position x_s of the shock and the value of M_1 have been defined by the intersection of tangents to the surface-pressure curves as sketched in Fig. 2.

***It was found for the aerofoil tests analysed in Ref. 1 that the shock was just strong enough to cause separation of a turbulent boundary layer when M_1 reached a value given approximately by the straight line joining the points ($M_0 = 0{\cdot}7$, $M_1 = 1{\cdot}26$), ($M_0 = 0{\cdot}9$, $M_1 = 1{\cdot}22$).

The significance of the movement of the shock on the lower surface and of the occurrence of sonic pressure at the trailing edge, both shown in Figs. 3–5, will be discussed below (Section 3.1.).

Values of $C_{pT.E.}$* obtained for nearly constant Mach numbers and varying normal force are plotted against aircraft normal force coefficient, C_{N_A} in Figs. 6 and 7 for the *X*–1–2 and *D*–558–I aircraft respectively. For an intermediate range of speeds, $C_{pT.E.}$ diverges from its very slow variation at a certain normal-force coefficient which decreases with increasing Mach number. This is again most probably due to the occurrence of shock-induced separation when the shocks become strong. The divergence of $C_{pT.E.}$ shows up rather more clearly, however, if it is cross plotted against M_0 for constant values of C_{N_A}. This is done in Figs. 8a to e for the X–1–2 and Figs. 9a to e for the D–558–I. The values of the local Mach number, M_1, just upstream of the shock are also included, again obtained by cross plotting. It should be emphasized that although discrete values are indicated by symbols, these are not actual experimental observations but values read from curves such as those in Figs. 6 and 7. The symbols have been included to demonstrate that there is some freedom in drawing individual curves. As drawn, and the aim has been to make them consistent with one another, they suggest that the free-stream Mach number at which $C_{pT.E.}$ diverges from its smooth rise agrees quite well with that at which M_1 reaches the value observed for separation on aerofoils, except for $C_{N_A} = 0{\cdot}6$ on the X–1–2 (Fig. 8c) and for $C_{N_A} = 0{\cdot}7$ and $0{\cdot}8$ on the D–558–I (Figs. 9d and e).

The agreement between the local conditions in flight for the divergence of $C_{pT.E.}$ and hence, most probably for separation, with those for turbulent separation on aerofoils in wind-tunnel tests is encouraging as far as it goes. It must, however, be remembered that the results are for one station only on each aircraft near the centre of the span, and that agreement is likely to be less good near the wing-fuselage junction and the tip. Moreover, none of the aircraft so far considered has swept wings. Again, the analysis has been restricted to the range of C_L in which the separation occurs downstream of the leading edge.

The Mach number for the divergence of $C_{pT.E.}$ is plotted against aircraft normal-force coefficient in Fig. 10a and b for the X–1–2 and D–558–I aircraft respectively. The buffet boundaries are plotted for comparison (*see* Section 4.2).

2.2. *Wind-tunnel Pressure-plotting Tests on Swept Wings.*

Very few detailed observations of surface pressures and flow patterns have been made on swept wings with the boundary layers turbulent in the region where they interact with the shock waves. In order to be able to consider the component of the local Mach number normal to the shock front, observations of the shock front and of the local flow direction are needed as well as the pressure distributions. The report on the RAE tests on the Hawker P.1052[10] gives valuable detailed pressure distributions but no visual observations of the flow, whereas the converse is true of information available on the Vickers Type 1000 wing.

The planform of the Hawker P.1052 is sketched in Fig. 11, showing the four pressure plotting stations and the position of the transition thread. Typical curves of $C_{pT.E.}$ plotted against Mach number for constant incidence are shown in Fig. 12 for the four stations. It is most probable that the divergence of $C_{pT.E.}$ again indicates the occurrence of separation. The free-stream Mach number at which the divergence occurs is plotted against wing lift coefficient in Fig. 13 for all four stations. Parts of the curves, for high C_L and low M, are shown broken because the divergence is less well defined in this region, and because the separation occurs fairly near the leading edge and might therefore behave differently from that considered so far, especially if it starts near or upstream of the transition thread. It is most noticeable that the divergence, and hence by assumption separation, occurs earlier for the outboard stations if C_L is above $0{\cdot}2$ or M_0 below $0{\cdot}85$. For low Mach numbers, up to about $0{\cdot}75$, this is due to an early separation near the leading edge and seems to be associated[10] with more severe adverse gradients immediately downstream

---

*The C_p plotted in Figs. 6 to 9 was measured not quite at the trailing-edge but at $0{\cdot}97c$ on the upper surface for the X–1–2 aircraft and at $0{\cdot}99c$ on the upper surface for the D–558–I aircraft.

of the peak suction. For Mach numbers in the region of 0·8, however, the supersonic flow and favourable gradients have extended downstream with a corresponding rearward movement of the shocks and separation points. The earlier separation is now no doubt due to the existence of appreciably higher local Mach numbers over the outboard part of the wing.

Shock positions as defined in Fig. 2 have been found for $\alpha = 0,2,3$ and 5 deg and approximate shock fronts determined from these. The values of the component local Mach number normal to and just upstream of the shock front, $M_1 \cos \theta$,* when $C_{pT.E.}$ diverges from its slow rise are tabulated in Table 2 below. In the absence of more accurate information it is assumed that the flow direction ahead of the shock is parallel to the free stream.

TABLE 2

Mach Numbers Ahead of the Shock on the P.1052 Wing.

Station	α	M_0 for divergence of $C_{pT.E}$	$M_1 \cos \theta$	M_1	Local Mach number for separation on aerofoils
$2y/b = 0{\cdot}96$	0°	$0{\cdot}90_5$	1·34		1·22
	2°	0·88	1·30		1·22
	3°	0·81	1·18		1·24
$2y/b = 0{\cdot}79$	0°	$0{\cdot}89_5$	1·22		1·22
	2°	$0{\cdot}87_5$	1·26		1·22
	3°	0·83	1·27		1·23
	5°	$0{\cdot}80_5$	1·23		1·24
$2y/b = 0{\cdot}48$	0°	$0{\cdot}89_5$	1·17	1·21	1·22
	2°	0·86	1·15	1·21	1·23
	3°	0·85	1·14	1·20	1·23
	5°	0·83	1·23	1·25	1·23
$2y/b = 0{\cdot}212$	0°	0·91	1·19	1·19	1·22
	2°	$0{\cdot}87_5$	1·10	1·14	1·22
	3°	$0{\cdot}85_5$	1·11	1·12	1·23
	5°	$0{\cdot}83_5$	1·09	1·11	1·23

The station at 0·79 semi-span is the only one for which there is reasonable agreement between the values of $M_1 \cos \theta$ and the value of local Mach number observed for separation on two-dimensional aerofoils[1]. Some, but by no means all of the discrepancy might be due to inaccuracies in the determination of the angle of the shock front or in the assumed flow direction; at the 0·48 semi-span station, for example, the full resultant local Mach number would have to be used to obtain agreement with the aerofoil observations. Moreover, the divergence of $C_{pT.E.}$ at 0·21 semi-span occurs for comparatively low resultant local Mach numbers. It is clear, therefore, that the conditions for shock-induced separation on some parts at least of swept wings are different from those on two-dimensional aerofoils. Further investigations of these conditions are needed and also of how the pressure rise across the shocks depends on their geometry and the local flow directions.

The value of visual observations of shock fronts and boundary-layer separation in any such investigation is demonstrated by the results on the Vickers Type 1000 wing. Oil on the surface gives a good indica-

*θ is the acute angle between the shock front and free-stream direction.

tion of the position of the shock front and also of when separation occurs. The Mach number-incidence boundary for separation at the front of the shock, as determined by oil and tufts, is reproduced in Fig. 14b and can be correlated with the occurrence of certain 'steady flow' changes in the forces and moments on the wing. (*See* Section 3 below and Fig. 14a.) No reversed flow was observed near the root section.

Changes of $\partial C_N/\partial\alpha$ and of $\partial C_m/\partial C_N$ similar to corresponding changes for the Vickers Type 1000 wing were observed on a 35 deg swept wing in the Ames 16 high speed tunnel[13] at a Reynolds number of $4{\cdot}6 \times 10^6$, as shown in Fig. 15a for example. It is suggested in Ref. 13 that the boundary layers were turbulent at the shock waves for this Reynolds number, but no observations of the transition point were made. The results are relevant to the present discussion, however, even if there is some doubt about transition position because the changes in sectional $\partial C_n/\partial\alpha$ and $\partial C_m/\partial C_N$ occur for much lower values of wing normal-force coefficient for outboard stations, Fig. 15b, than for inboard ones, suggesting that separation occurs earlier outboard. There are in fact no abrupt changes for the innermost stations. The pressure distributions reveal that, as for the Hawker P.1052 wing, the local Mach numbers were higher for the outboard stations, which could account for earlier separation there.

The observations on these three swept wings suggesting that separation occurs earlier or that its effects are more severe for outboard stations than for inboard ones have an important bearing on the 'pitch-up' problem (*see* below). It is also of interest and probably relevant that for two of the wings there were little or no signs of separation near the wing-root.

2.3. *NACA Flight Tests with Vortex Generators.*

Several such tests have been described and will be reviewed briefly in the discussions on vortex generators in Section 5.4. Two reports of special interest are mentioned at this stage because they illustrate further methods by which separation has been detected in flight. On the F–86A (Sabre) aircraft[11] an abrupt up-float of the ailerons, Fig. 20a, was found, by observing tufts, to be associated with separation and was thus a convenient 'detector'. In addition, a good indication of the severity of the separation can be obtained from records of the magnitude of the floating angle. The tests on the F–86A aircraft will be referred to repeatedly because the delay in the occurrence of separation (*see* Fig. 20b) due to vortex generators and other devices and the reduction in its severity (Fig. 20a) can be correlated with improvements in the 'pitch-up', wing dropping and buffeting tendencies of the aircraft (see below). The presence of reversed flow at the trailing edge of the F–51D aircraft[12] was detected by boundary-layer traverses at that position (*see* Fig. 41).

3. *Examples of the Effects of Shock-induced Separation on 'Steady-flow' Aerodynamic Characteristics.*

3.1. *Shock-wave Movements and Section Forces and Moments.*

The mechanism by which separation exerts a strong influence on the movement of the shock waves and hence on the development of the regions of low-pressure supersonic flow on two-dimensional aerofoils is discussed in Ref. 1. The divergence of the pressure at the trailing edge from its smooth and gradual variation is regarded as a key factor in this mechanism because it tends to disturb the equality, or near equality, of pressure on the two sides of the wake at the trailing-edge position which must be maintained for steady flow. The fall in trailing-edge pressure is counteracted by a deceleration in the development of the flow, i.e. in the rearwards shock-movement, on the surface where the separation first occurs* and an acceleration in the development of the flow on the other surface. Precisely the same mechanism is evident for sections of finite wings in Figs. 3 to 5 and must react on the sectional forces and moments in the same way as on those for two-dimensional aerofoils[1]. The further change which occurs in the relative shock movements when the pressure at the trailing edge becomes sonic is also shown by Figs. 3 and 4. An abrupt supersonic expansion can now occur at the trailing edge, on the lower surface, to maintain the equality of pressure there; thus an overall effect on the flow is no longer necessary to counteract the reduction in pressure on the upper surface. The upper surface shock moves rearwards again and the lower surface one slows down.

*The upper surface for an aerofoil or wing producing positive lift.

An example of the effects on section characteristics is seen in the variation of section centre of pressure, Fig. 16, derived for the X–1–1 and X–1–2 aircraft from the same tests as the data shown in Figs. 3 and 4. The fairly violent forward movement of the centre of pressure corresponds to the nose-up changes in pitching moment shown for constant C_L's on a two-dimensional aerofoil in Fig. 33c of Ref. 1, and is due mainly to the rapid rearward movement of the lower-surface shock at a stage when the upper-surface one is almost stationary. The centre of pressure moves back again when the pressure at the trailing edge falls below the sonic value.

There are no direct results from the flight tests under consideration on the effects of separation on section lift coefficient at constant incidence or with constant control deflection, but they clearly must be similar to those producing the characteristic trough in the C_L *vs.* M curves obtained on aerofoils. The trough shows up also in $\partial C_L/\partial\alpha$ and control effectiveness. Loss of normal force on some part of the wing or tailplane, either of that due to incidence or that due to control deflection, is in fact responsible for the examples of undesirable 'steady-flow' phenomena discussed below.

3.2. *Control Effectiveness.*

Troughs similar to those observed in the variation of control effectiveness with Mach number for two-dimensional aerofoils occur also for finite wings if the design is such that shock-induced separation occurs. As discussed in Ref. 1 the reason is basically, if a fixed control setting is considered, that the separation causes relative shock movements similar to those observed on plain wings, *see* Figs. 3 to 5 for example, but aggravated by the changes in surface slope at the flap hinge. Alternatively, a change of flap deflection for a fixed Mach number can be considered. Firstly suppose the shock on one surface is causing separation upstream of the hinge, then deflection of the flap away from that surface increases the depth of the dead-air region and hence tends to reduce the pressure recovery along the flap instead of increasing it as it would do in the absence of separation; the opposite tendency will occur simultaneously on the other surface if the flow is separated there also. The changes in shock position produced by the flap deflection are small or even in the opposite sense to that desired. Secondly, if the shock on the surface is on the flap, deflection of the flap away from this surface will increase the local Mach number upstream of the shock, which will either cause the flow to separate or, if it has already done so, increase the severity of the separation. The opposite tendency will exist simultaneously on the other surface if that shock also is already on the flap. The net result is again that the shock movements produced by the flap are either small or in the opposite sense to that desired.

Aileron effectiveness measured[14] for the X–1–2 (XI) aircraft at an altitude of 40 000 ft* is shown in Fig. 17. Although the curve is not defined between 0·82 and 0·9 the trough is clearly present above this. The effectiveness falls nearly, if not quite, to zero.

A difficulty in comparing aileron effectiveness measured in piloted aircraft with that measured in wind tunnels or on ground-launched rockets arises because flight results are averages for fairly large ranges of deflection in which the variation is non-linear, the effectiveness being less for the small deflections. This is illustrated, for example, by the tests on the Sabre[11]. Aileron effectiveness, averaged for 12 to 16 deg deflection and obtained at 35 000 ft* altitude, is shown by the curve in Fig. 21 and falls almost but not quite to zero at $M_0 = 0{\cdot}96$. Records obtained during 'wing-dropping' tests on this aircraft (*see* below) revealed, however, that a very definite reversal in effectiveness occurred for small deflections[11]; rolling velocities in the opposite sense to the applied aileron deflection were recorded through several reversals of direction. On this aircraft vortex generators caused a small improvement in effectiveness (*see* below) which might be slightly more than suggested by Fig. 21 because the results for generators were averaged over a smaller range of flap deflections than those for the plain aerofoil.

A further example of the loss in aileron effectiveness measured in a piloted aircraft is shown in Fig. 27. This was measured on a straight-wing jet aircraft[15] with a 12 per cent thick wing and was used in an analysis of the 'wing-dropping' of the aircraft (*see* below).

*The loss due to aero-elastic effects would presumably be small at this altitude.

Interesting results for the effectiveness of an all-moving wing tip on a 10 per cent thick swept wing have been obtained in ground-launched rocket tests at the R.A.E.[16], and are reproduced in Fig. 19. A marked trough in the effectiveness curve occurred between $M_0 = 0{\cdot}9$ and $1{\cdot}0$ for the NPL 304 section (10 per cent thick). This was most probably due to shock-induced separation especially since it started at about the same Mach number as the loss in rolling effectiveness for the complete wing at incidence. The trough was even more marked for RAE 104 section (10 per cent thick) and this may be due to the smaller nose radius which leads to higher local Mach numbers.

The results of numerous ground-launched rocket tests on flap controls, as described for example in Ref. 17, are also broadly consistent with the findings that the effects of separation are less severe for sections with small changes in slope over the rear and with small trailing-edge angles.

3.3. *Longitudinal Stability of the* X–1–1 *and* X–1–2 *Aircraft.*

A detailed analysis of the longitudinal stability and trim of these aircraft is given in Ref. 18 for $C_L = 0{\cdot}3$, approximately the condition for the data given in Figs. 3 and 4. The variations are bound up with the effectiveness of the stabiliser-elevator combination, and cannot, therefore, be fully correlated with the effects of separation because no data are available to show when separation occurred on the tailplane. Curves of $\partial C_L/\partial\alpha$ for the complete aircraft are reproduced here in Fig. 18a. They show that the occurrence of the first drop, and of the recovery from the trough, correlate reasonably well with the occurrence of separation on the wing and sonic pressure at the trailing edge for the single stations represented in Figs. 3 and 4. The analysis demonstrates that the major part of the variation of the static stability of the X–1–1 aeroplane (Fig. 18c) was the contribution of the horizontal tail, and that this in turn was related to the variations in rate of change of downwash with incidence, $d\varepsilon/d\alpha$ (Fig. 18b). The onset of the loss of downwash and of the subsequent partial recovery coincide with the similar changes in $\partial C_L/\partial\alpha$, and were almost certainly associated with separation on the wing. In general, the effects of changes in downwash will depend very much on the position of the tailplane.

3.4. *'Pitch-up' Instability of Swept-back Wings.*

Several investigations on aircraft with swept-back wings, *see* for example Refs. 11, 19, 20, 21, have reported an 'instability boundary' limiting the manoeuverability, or usable C_L, to a value which decreases with increasing Mach number. The nature of the instability is often[11] 'a reversal in the variation of elevator stick force and position with normal acceleration which makes it difficult to attain higher accelerations without overshooting or inadvertently pitching up to a stall'. In the tests described in Ref. 21 the turns performed with the use of the elevator alone, i.e. stabilizer fixed, were described as being of an 'uncontrollable nature' when 'pitch-up' occurred. The 'instability boundary' of this aircraft, the D–558–II (35 deg swept wing, with 10 per cent thickness at root and 12 per cent at tip), is reproduced in Fig. 28 and the peak normal-force coefficients reached in the pitch-up are indicated. These show that very high loads can inadvertently be reached, and illustrate the potential danger of the pitch-up should it occur at low altitudes*.

---

*It is suggested in Ref. 21 that these values of C_{N_A} are in fact the maximum attainable. This type of variation with Mach number follows fairly closely that of $C_{L\,\max}$ for two-dimensional aerofoils, and the upward trend at the higher Mach numbers might be the rise which occurs when sonic pressure is reached at the trailing edge and the upper-surface shock starts moving rearwards again[22]. This would seem a plausible explanation of an accident to a Swedish aircraft of which we have had a brief verbal description. The aircraft apparently broke up as a result of excess loads in a pitch-up. The fact that the upper-surface shock had moved far back along the chord during the manoeuvre was deduced from the presence of skin wrinkling there, which could only be accounted for by the occurrence locally of the low pressures associated with supersonic flow.

It is now widely accepted that separation and the resulting loss of lift outboard on the wings is responsible for the instability of the complete aircraft*. Some evidence to support this is collected below for the range of Mach numbers in which the offending separation is induced by shock waves downstream from the leading edge.**

For the flight tests described in Ref. 19 (F 86 A, Sabre aircraft) tail loads measured in pitch-ups at constant Mach numbers demonstrate, Fig. 22, that the change in variation of elevator angle is accounted for almost entirely by the deflection needed to balance the nose-up changes in pitching moment of the wing and fuselage. The pitching moments for the wing alone were obtained by pressure plotting. They show that the nose-up changes for the wing plus fuselage are almost exactly those for wing alone, Fig. 23, and hence it follows that the changes for the wing are the cause of the instability.

Similar abrupt nose-up changes in the variation of C_m with C_L for constant Mach numbers, i.e. positive values uf $\partial C_m/\partial C_L$, are frequently observed for swept-back wings. That for the Vickers Type 1000 wing, Fig. 14a, full-line. is typical and has been correlated with the occurrence uf shock-induced turbulent separation*** (*see* Fig. 14b). It is deduced in Ref. 19 from the wing pressure plotting data on the F 86 A (Sabre) aircraft that the destabilizing wing pitching moments arise because separation and loss of lift occur earlier and more severly on the outboard portions of the wing than inboard. This is illustrated in Fig. 24 in which the change in section normal-force coefficient with aircraft normal-force coefficient is shown for five spanwise stations. The centre of lift clearly must move inwards along the axis of the wing and hence forwards. These deductions are supported by the observations of the occurrence of separation for the three swept wings considered in Section 2.2 (*see* Figs. 13, 14 and 15). For two of these there were little or no signs of separation near the root sections and when it did occur there for the third (Hawker P.1052), its effects were probably less severe than for sections further outboard, judging from the smaller effect on $C_{pT.E.}$ (*see* Fig. 12). It is possible that the greater proneness to separation for outboard stations is aggravated for the D 558 II aircraft[21] by its increase in section thickness from the root to the tip (10 per cent to 12 per cent). The importance of the pitch-up problem and its association with the redistribution of the wing loading which results from the variation in the occurence and severity of separation along the span would seem to merit a thorough investigation, on a swept wing with turbulent boundary layers, of the basic reasons for this variation; the presence of higher local Mach numbers outboard is no doubt an important factor.

The close connection between separation and pitch-up is further demonstrated by the delay in the destabilizing changes which were achieved by the use of vortex generators on the Sabre wing[11], Fig. 25a. The variation with Mach number of the normal force at which the instability occurs is shown in Fig. 25b. The use of fences (*see* Section 5.5) gave a slightly greater delay than vortex generators.

3.5. *Wing Dropping.*

The wing-dropping tendency occurs at transonic speeds for both straight and swept-back wings, and makes itself felt by the rapid increase in the aileron deflection required to hold the wings level. Evidence that the tendency is associated with shock-induced separation is provided by the result that vortex generators placed at 0·35 chord of the wing of the F–86–A (Sabre) aircraft[11] drastically reduced, if not eliminated, wing dropping for this aircraft. Some of the measurements made of aileron angle for various

---

*The nose-up changes in section pitching moment such as observed in Ref. 15 must also contribute to the nose-up change in wing pitching moment.

**The instability often occurs at low Mach numbers but at higher lift coefficients, due to earlier or more intensive stalling outboard than inboard. In an intermediate range of speeds this stalling must be influenced by compressibility effects near the nose.

***The broken line in Fig. 14a has been included to show that the nose-up change is not necessarily revealed by results obtained when the boundary layer is laminar in the region of its interaction with the shock waves (*see* also Fig. 15a).

rudder forces, i.e. various degrees of sideslip, are reproduced in Fig. 26. The favourable effect of the generators can only have resulted from suppressing a separation, or from reducing its effects. Vortex generators on the wing of the D–558–I aircraft delayed the onset of wing dropping from a Mach number of about 0·84 to one of about 0·89.

The wing dropping presumably arises because of differences in the occurrence and effects of separation on the two wings, which can be due to inherent asymmetry or can be induced by certain asymmetrical manoeuvres such as sideslip.

The results in Ref. 23 show that the wing-dropping tendency is due to a simultaneous loss in aileron effectiveness, and an increase in the out-of-trim rolling moment, i.e. the rolling moment due to sideslip. Figs. 27a and b are reproduced to illustrate this.

It was not possible to determine how much of the improvement caused by the generators on the F–86–A (Sabre) aircraft was due to an increase in aileron effectiveness, and how much to a reduction in $\partial C_l/\partial\beta$, the rolling moment due to sideslip. The aileron effectiveness with and without vortex generators, Fig. 21, cannot be compared directly because the total deflections were different (*see* above). There is, however, still a marked reduction in aileron effectiveness at $M_0 = 0{\cdot}96$. This suggests that the reduction in the out-of-trim rolling moment was the more important factor.

Results from a systematic investigation,[24] by a ground launched rocket technique, of the effects of section shape, thickness, sweep, etc., on the occurrence of wing dropping show trends which are consistent with qualitative deductions which can be derived by assuming that separation is the cause of wing dropping. For example, it was found that sections of 6 per cent thickness or below did not exhibit wing dropping, with the exception of a 6 per cent double-wedge aerofoil which would have high local Mach numbers just downstream of the shoulder.

4. *Examples of the Connection between Shock-induced Separation and Buffeting.*

Although most writers on high-speed buffeting agree that it is frequently associated with shock-induced separation of the boundary layers, the evidence which they cite in support of this view is surprisingly meagre. This is because very few complete or systematic sets of observations have been made. In many cases where detailed observations of buffeting have been made, correlation with the onset of flow separation is not possible because of the absence of pressure distributions or other information on the flow near the wing. In some experiments, for example, elaborate measurements of the pressure fluctuations on the wing and in the wake have been made without measuring the mean pressure distribution on the wing.

In the following paragraphs the available data on the flow phenomena which give rise to high-speed buffeting are briefly reviewed and, where possible, an attempt is made to show the importance of shock-induced separation. Since buffeting arises either from the effects on the tailplane of fluctuations in the wake of the wing, or from the associated* fluctuations in the loading on the wing itself, the available information on these matters will be considered first.

4.1. *Observations of the Fluctuations in the Wake or in the Pressure Distribution on the Wing.*

A number of wind-tunnel experiments have been reported in which the boundary layer on the wing was laminar ahead of the shock waves. In some of these[25] the fluctuations in the wake have been detected by using strain gauges to observe the vibration of a small aerofoil held downstream of the wing, and in others[26,27,28], the pressure fluctuations at the surface of the wing and the associated oscillations of the shock waves have been observed.

The measurements reported in Ref. 26 are of considerable fundamental interest although they should be applied with care because of the low Reynolds number of the experiment. The fluctuations in static pressure were measured at several points on the surface of a family of two-dimensional aerofoils. At low incidences the fluctuations were found to consist of bursts of roughly constant-frequency, constant-

*For example (as suggested in Ref. 1) any fluctuation in the pressure at the trailing edge of the wing will produce fluctuations in the positions of the shock waves so long as the flow at the trailing edge remains subsonic.

amplitude oscillations separated by intervals in which the fluctuations were of a random nature. It was found that for the constant-frequency type of oscillation the product of the frequency and the chord was roughly constant, and that this was also true for unpublished results obtained at considerably higher Reynolds numbers (up to 5×10^6). It is argued that the amplitude of the constant-frequency oscillation is most representative of the force fluctuations which cause buffeting at low incidence. At high incidence the pressure fluctuations were found to be of a more random nature but there were pulsations, usually of an intermediate amplitude, which appeared to predominate and these were taken as typical for the purpose of analysis. In the diagrams reproduced here, the amplitude Δp of the pulsation is expressed in non-dimensional form by dividing by the dynamic head of the undisturbed stream. For moderate and high incidences the amplitudes of the pulsations on the upper surface were much larger than those on the lower surface, and curves for the upper surface only are included. Typical records are shown in Figs. 29a and b where the amplitude is plotted for a range of free-stream Mach numbers against distance along the chord for two symmetrical aerofoils (one 12 per cent thick and the other 4 per cent thick), and for a small angle of incidence (1·6 deg) and a fairly large angle of incidence (6·4 deg).

For the thicker section at small incidence, the fluctuations of pressure are roughly uniform along the chord at Mach numbers below the critical (*see* curve for $M_0 = 0{\cdot}70$). These fluctuations are probably associated with disturbances arising from laminar separation over the rear of the aerofoil. At $M_0 = 0{\cdot}80$ the fluctuations rise rapidly to a maximum at about 0·45 chord and then fall again. An examination of the schlieren photographs reproduced in Refs. 26 and 29 suggests that for the type of curve described above the maximum occurs in the region between the point of laminar separation and the shock. The subsequent fall of amplitude may be associated with reattachment of the separated layer after transition to turbulent flow has taken place. As the Mach number is raised (*see* Fig. 29a) the peak in the amplitude curve moves rearwards, following the rearward movement of the shock and separation point. At the higher Mach numbers there is little fall of amplitude behind the peak, and this may be associated with the fact that the boundary layer then no longer reattaches to the surface after separating ahead of the shock. When the Mach number approaches unity the shock and the separation point have moved back close to the trailing edge, and the pressure fluctuations are then small.

Fig. 29b shows that at low incidence the pressure fluctuations are reduced considerably by using a thin section. This is presumably because the peak local Mach number is reduced thus alleviating the tendency for separation to occur; the height of the separated region is also reduced and this may reduce the scale of the disturbances formed after separation.

At a larger incidence the pressure fluctuations on the thin section are, however, larger than for the thick one. For the thicker section the general shapes of the curves (Fig. 29a) are the same as at low incidence, but for the thin section there is a peak in the amplitude near the nose at the lower Mach numbers. The schlieren photographs of Ref. 29 show that this peak is probably associated with flow separation from the leading edge. Between $M_0 = 0{\cdot}7$ and $M_0 = 0{\cdot}8$ the flow attaches to the nose, and the separation point moves downstream with the shock. The pressure fluctuation curves are then of similar shape to those for low incidence.

These results suggest that at small lift tendency for buffeting to occur can be alleviated by a reduction of the aerofoil thickness, but that at high lift buffeting may at some Mach numbers be aggravated by the use of thin sections. In a later report[27] the effects of camber, and a nose flap on buffeting associated with leading-edge separation are considered. It is shown that both are effective, and this is illustrated by the comparisons shown in Fig. 30.

Although the direct application of the results of these experiments is probably not possible because of the scale effects arising from the use of laminar boundary layers, there is little doubt that qualitatively similar results would be obtained under full-scale conditions. Smaller pulsations might be expected at low Mach number, and the peaked type of curve would probably not occur until a rather higher Mach number was reached. Also, since reattachment does not usually occur after a turbulent separation on an aerofoil, it might be expected that there would in general be no large fall of amplitude downstream of the peak.

Measurements of the pressure fluctuations at a higher Reynolds number (9 to 11×10^6) are reported in Ref. 28. The fluctuations of total head were observed in the wake behind a two-dimensional aerofoil of NACA 23013 section at Mach numbers up to 0·8, and a limited number of measurements of the static pressure fluctuations at the surface of this aerofoil and an aerofoil of NACA 25_1–213 section are also given. A few observations of the fluctuations of the direction of flow in the wake of the 23013 section are included.

It was found that the total-head fluctuations in the wake 0·7 chord behind the trailing edge of the 23013 section never extended outside the average boundaries of the wake, and that the fluctuations had maxima where the gradients of the mean total-head loss were a maximum. These features are illustrated in the results for $\alpha = 2$ deg reproduced in Fig. 31. At low angles of incidence the amplitudes of the maximum total-head fluctuations were little greater than those of the average total-head fluctuations shown in Fig. 31. With increase of incidence, however, the maximum amplitude increased more rapidly than the average, and in some cases approached the mean total-head loss in the wake. This is illustrated in Fig. 32 where the average and maximum amplitudes are plotted for $\alpha = 5$ deg and $M_0 = 0{\cdot}75$.

The largest amplitudes of the average total-head fluctuations in the wake are plotted against Mach number for a range of angles of incidence in Fig. 33. It is seen that as the Mach number is raised the amplitude at first remains substantially constant, but begins to rise rapidly at a value of the Mach number which depends on the incidence. Some of the curves show also that the amplitude begins to fall again at higher Mach numbers. As suggested in Ref. 1 this might be expected because the rearward movement of the shock and separation point should lead to a reduction of the scale of the disturbances in the wake.

In Ref. 28 a buffet boundary is defined by cross plotting the points where the slopes of the curves shown in Fig. 33 first reach 0·1 ; these points are indicated in Fig. 33, and the corresponding buffet boundary is reproduced in Fig. 34. An alternative method for defining a boundary for tail buffeting is to show the values of the lift coefficient and Mach number at which the tailplane first enters the region of unsteady flow in the wake. Such a boundary is reproduced in Fig. 34, the position of the tailplane being chosen to correspond as closely as possible to that of the F8F aeroplane. The wing section of this aeroplane is not NACA 23 013, but is 23 018 at the root and 23 009 at the tip; the tailplane is 1·03 chord behind the wing instead of 0·70 chord as in the experiment. In spite of these differences, however, the trends of the flight-determined buffet boundary and the buffet boundaries predicted from the wind-tunnel tests are similar; this suggests that the buffeting encountered in flight was closely connected with the appearance of large-amplitude disturbances in the wake of the wing or with the associated fluctuations at the wing surface.

The frequencies of the total-head fluctuations in the wake were found to be of a random nature unless a periodic fore and aft oscillation of the shock waves occurred. When this happened the frequency of the shock oscillation could sometimes be detected in the wake. When shock oscillation occurred the pressures at all points on the surface of the aerofoil were found to oscillate at about the frequency of the shock, but with a difference of phase.

The experiments described above show that large-amplitude fluctuations of the flow at the aerofoil surface and in the wake may begin at a free-stream Mach number above the critical, and fall off considerably before a free-stream Mach number of unity is reached; this is in qualitative agreement with the simple explanation advanced in Ref. 1. Considerable difficulty arises, however, in attempting to correlate the beginning of the rapid rise of amplitude with the onset of shock-induced separation of the boundary layer because inadequate data are available on the mean flow near the aerofoils. The amplitude certainly rises rapidly at about the same conditions as separation would be expected to occur, and there is some indirect evidence (e.g. the effect of aerofoil thickness) which suggests that there is a close correlation between separation and the growth of the pressure fluctuations.

4.2. *The Correlation between Flight-determined Buffet Boundaries and Shock-induced Separation.*

Further indirect evidence on the correlation between buffeting and shock-induced separation of the turbulent boundary layers is contained in the results reported in Ref. 30. Here the flight-determined buffet boundaries of eight straight-winged aircraft are compared with the results given by five methods of predicting the buffet boundary. One of these methods is based on the critical Mach number for the

wing section and, as would be expected, gives results which bear little consistent relation to the observed Mach numbers at which buffeting begins, but the other methods give better agreement and all bear some relation to the Mach number at which shock-induced separation might be expected on the wing section. For example, one method is based on the Mach number at which the lift curve (plotted against Mach number) reaches its peak, and another on the Mach number at which the rate of lift-increase begins to fall just before the peak is reached. It is shown in Ref. 1 that both of these features are connected with the onset of boundary-layer separation.

A comparison between the flight-determined buffet boundaries of two swept-wing aircraft and the predictions of the methods described above is also given in Ref. 30. In general the agreement is found to be less satisfactory than for the straight-wing aircraft.

In order to obtain a more direct comparison between the conditions under which buffeting and boundary-layer separation begin, a search has been made for examples in which both the flight buffet boundary and the wing pressure distribution have been measured. The examples which have been found have all been mentioned above in other connections.

Values of the Mach number and normal-force coefficient at which buffeting was first observed in flight on the X–1–2 and D–558–I aircraft are shown on the curves of $C_{pT.E.}$ reproduced in Figs. 6 and 7. For the D–558–I aircraft (Fig. 7) two buffet boundaries have been reported; these are in reasonable agreement at the lower Mach numbers, but differ seriously when the Mach number is raised. It is not known whether this discrepancy arises from differences between the aircraft on which the boundaries were measured*, or from differences in the techniques used to determine the boundaries.

It is seen in Fig. 6 (X–1–2 aircraft) that for Mach numbers between 0·62 and 0·75 there is good agreement between the buffet boundary and the points at which the trailing-edge pressure begins to fall rapidly (i.e. at which separation occurs at the shock). At Mach numbers of 0·8 and 0·82, the trailing-edge pressure is already falling rapidly before buffeting is observed, and it is concluded that buffeting did not occur until appreciably after separation first took place at the shock. This feature is shown more clearly in Fig. 10a where the results of Fig. 6 have been cross plotted; it is seen that the discrepancy between the buffet boundary and the curve showing the conditions under which $C_{pT.E.}$ begins to diverge rapidly from a nearly constant value increases rapidly at the higher Mach numbers.

The results for the D–558–I aircraft shown in Figs. 7 and 10b show similar trends to those discussed above for the X–1–2, except that the situation is complicated by the uncertainty arising from the existence of the two buffet boundaries.

The only swept-wing aircraft for which a detailed comparison is possible between the buffet boundary and the onset of shock-induced separation is the P.1052. Here the buffet boundary has been determined in flight, and the conditions under which separation occurs can be estimated from wind-tunnel tests made with transition to turbulent flow in the boundary layer fixed near the leading edge. Curves showing the Mach numbers and lift coefficients at which $C_{pT.E.}$ begins to diverge from its smooth variation with Mach number are reproduced in Fig. 13 for four spanwise stations, and the buffet boundary is included for comparison. The agreement with the buffet boundary is good for the inboard stations, but it is clear that extensive separation is present near the tip before buffeting is observed (*see* also Section 2.2).

Indirect evidence on the connection between shock-induced separation and buffeting is contained in the flight tests on the F–86A–5 aircraft reported in Ref. 13. Here the sudden change which occurs in the aileron floating angle (*see* Section 2.3 and Fig. 20a) is thought to indicate the onset of shock-induced separation of the boundary layer. The conditions under which this sudden change occurs are compared in Fig. 20b with the buffet boundary, and reasonable agreement is found up to a Mach number of about 0·9. This diagram also shows the beneficial effect of vortex generators, and this is discussed in the next Section.

*If this is so the values shown by the full lines in Fig. 7 provide the most valid comparison because they were obtained on the aircraft used for the pressure measurements.

5. *Some Methods for Preventing Shock-induced Separation or for Alleviating its Effects.*

5.1. *Introduction.*

Further information is discussed on certain of the methods briefly mentioned in Ref. 1. Other methods not mentioned in Ref. 1 and having particular application to sweptback wings are also now considered.

The sketches in Fig. 35 illustrate how the occurrence of separation at the foot of a shock on an aerofoil influences the pressure at the trailing edge of the aerofoil. The overall pressure recovery from a point just upstream of the shock to the trailing edge consists of two parts, namely AB, the compression through the shock, and BC, the subsonic recovery from immediately downstream of the shock to the trailing edge. Separation reduces both parts and most of its effects on the 'steady-flow' characteristics can be traced to this reduction in pressure recovery[1]. The full recovery should be obtained if the separation is eliminated as is demonstrated by Dr. Seddon's application of boundary-layer bleed on supersonic intakes (*see* Fig. 53 of Ref. 1). Even a partial restoration of the recovery is likely to be worthwhile, however, such as might be achieved by a reduction in the severity of the separation.

It should be possible to avoid shock-induced separation for moderate incidences and control deflections by suitable design of wing section and planform. High local Mach numbers will still occur, however, for large incidences or control deflections so that 'remedial' devices to suppress separation or to minimize its effects may still have some application on future aircraft. A wide and important field of application clearly exists for any such devices as can be developed for incorporation on current aircraft.

5.2. *Design of the Wing Section and Planform.*

As discussed in Ref. 1, the amount of supersonic expansion must be kept small (i.e. local Mach numbers below about 1.2) in order to avoid separation, which means that the change in surface slope downstream of the sonic point must be kept small. It was suggested that a section shape with small change of slope downstream of the shock and small trailing-edge angle, i.e. low rate of subsonic pressure recovery at the rear of the aerofoil, would also tend to minimize the effects of separation if it did occur. Unfortunately no further section data obtained with boundary layers turbulent at the shock waves have become available. Results obtained at the N.P.L. for the 6 per cent thick RAE 104 section with transition fixed and free illustrate, Fig. 36, that transition-free data can be misleading. Although laminar separation occurred on this aerofoil with transition free, the effects were less severe than those of the turbulent separation. The trough in the C_L *vs.* M curve is absent and also the violent forward movement of the centre of pressure position. From transition-free tests alone, therefore, this section might be wrongly assumed to be free of these undesirable characteristics.

Some NACA transition-free results are nevertheless reproduced from Ref. 31 to illustrate, qualitatively only, certain interesting effects of section thickness and of planform. To avoid the trough in the curve of $\partial C_L/\partial\alpha$ for a swept wing, Fig. 37a, and positive values of $\partial C_m/\partial C_L$ (Fig. 37b) it was necessary to reduce the wing thickness/chord ratio to 6 per cent if this was constant across the span, but they were absent also for a wing with 9 per cent t/c at the root tapering to 3 per cent at the tip. This is consistent with the observations recorded in earlier sections of the report that shock-induced separation is less prone to occur near the root of a swept wing than further outboard. Fig. 38 is a guide[31] to the way in which sweepback and low aspect-ratio can be used to minimize the effects of separation. Camber and twist can be employed on swept wings to eliminate large suction peaks which often occur near the wing tips at low speeds due to 'induced camber'[32]. The high local Mach numbers which occur at outboard stations at higher speeds, although further aft, probably arise from a similar cause and might therefore be reduced by similar methods.

Thin wings, sweepback and low aspect-ratio help to increase the forward Mach number for which separation first occurs even if they do not eliminate it. There may be some virtue in reducing at the same time the Mach number at which its effects begin to disappear again, i.e. that at which the pressure at the trailing-edge falls below the sonic value (*see* Figs. 3 and 4 and Section 3.1). An unswept trailing edge, i.e. delta planform, might help to do this.

Some remarks on the probable variation of section lift coefficient and centre of pressure in the absence of separation are relevant at this stage. The lift coefficient at constant positive incidence would tend to increase with Mach number until the upper-surface shock reached the trailing edge, whereupon an abrupt fall would occur to the 'supersonic' value. There would be no trough, but the fall would most probably be the more abrupt for having been delayed. For a section on which the lower-surface shock first formed upstream of the trailing edge the centre of pressure might move back beyond the 'supersonic' position, and then move abruptly but smoothly forward to that position once the upper-surface shock had reached the trailing edge. Some reduction in the abruptness of the changes could no doubt be achieved and instability avoided by suitable design of the planform.

5.3. *Suction or Blowing.*

One very successful application of suction has already been mentioned, namely the bleed upstream of a supersonic side-intake (*see* Fig. 53 of Ref. 1). Almost the full inviscid-flow pressure-recovery was obtained.

An experiment is described in Ref. 33 in which suction was used to suppress shock-induced separation in a nozzle formed by a bump on a wind-tunnel wall. Several arrangements of slots and one of a porous surface were used; those referred to here are sketched in Fig. 39. Separation was suppressed by all of these arrangements for all local Mach numbers up to the maximum reached on the bump, namely 1·40, but the pressure recovery varied from one to another. The best arrangement of slots was II, with five slots distributed both upstream and downstream of the shock, Fig. 40a. The results for this are interesting also in that the subsonic pressure recovery for the lowest speed shown is achieved through a series of steps at the slots and that a minimum pressure occurs upstream of each slot due to sink effect; the shock appears to jump from one slot to the next much as Sq. Ldr. Head has suggested it might[34]. The pressure recoveries for three arrangements of slots are compared in Fig. 40b. Comparison of II and VI suggests that not much is gained by sucking at slots upstream of the shock, but comparison of III with the other two suggests that there may be some advantage in having a slot located near the foot of the shock. Suction through the porous surface, V, gave a better rate of pressure recovery than the best slot arrangement, Fig. 40c. The porous surface extended both upstream and downstream of the shock and the compression at the surface is considerably 'softened', as presumably any abrupt pressure rise would be on a continuous porous surface.

This work should be extended to higher local Mach numbers, and applied to aerofoils where the movement of the shock relative to the slot positions is likely to be affected by the interaction between the two surfaces, and by the fact that large shock movements will occur on both surfaces when separation is suppressed on either. Multiple slots or porous surfaces on conventional sections are likely to give the best results. Griffith-type sections are unsuitable for high speeds because, even if the thickness were small, expansions to relatively high local Mach numbers would occur near the slot when separation was suppressed, leading to high wave drag and a greater tendency to separate at points downstream of the slot.

Blowing at the hinges of control flaps might prove effective as a means of improving the effectiveness of such flaps at high speeds.

5.4. *Vortex Generators.*

Vortex generators seem to have been first used by H. D. Taylor of the United Aircraft Corporation in the diffusers of low-speed wind tunnels to reduce or eliminate flow separation by increasing the mixing, and hence momentum transfer, in the boundary layer. Their possible application to problems involving shock-induced separation was soon realized in the U.S.A. and some early experiments done[35,12]. These gave promising results and, because the small vanes could readily be attached to the wings of existing test aeroplanes, were soon followed by further flight tests[11,36]. Several improvements in the behaviour of these aircraft have already been mentioned, including (i) on the North American F–86A (Sabre) aircraft[11], a delay in the occurence of 'pitch-up' (Fig. 25) and buffeting (Fig. 20b), a marked decrease in the wing-dropping tendency (Fig. 26) and a slight improvement in control effectiveness (Fig. 21); (ii) on the D–558–I aircraft[36], a delay in the occurance of wing dropping, and (iii) on the F–51D aircraft[12],

a delay in the occurrence of separation to a higher lift coefficient or Mach number (*see* Fig. 41). Two further applications designed to improve the pitching-moment characteristics of swept wings at high subsonic speeds have been reported from America. Generators at 0·15 chord produced no significant improvement in tunnel tests on a 45 deg sweptback wing[37] but they apparently have a beneficial effect in flight on the wing of the Boeing B.47 aircraft where they are placed further aft.* Where the drag increment due to the generators has been measured, it has been found to be quite small and in some cases negligible.

At the R.A.E., generators have been used upstream of a slide intake at supersonic speeds where they improved the pressure recovery[40] and on a sweptback wing at high subsonic speeds where 'no clear advantage was gained'. The first attempts at the N.P.L. to study the effects of generators on the flow over small two-dimensional aerofoils were unsuccessful, and so some work was initiated by L. H. Tanner in a small low-speed tunnel to study their design and mechanism. It was found that in order to be effective the vortices from the generators must, in two-dimensional flow at any rate, establish a flow pattern downstream of the generators similar to that sketched in Fig. 42 which shows contours of velocity in the boundary layer in a plane normal to the direction of flow (into the paper) and at an optimum distance downstream of the generators (considered here to be 'counter-rotating'**). The vortices carry air at the stream velocity down towards the surface in some parts of the span, AB, (i.e. between divergent blades of counter-rotating arrangements) and sweep air upwards away from the surface in the intermediate regions, BC (i.e. between convergent blades of counter-rotating arrangements). Since mixing with the boundary layer air must occur, the air swept away from the surface is partially 'de-energised'. The boundary layer is thinned considerably in the regions AB (in the N.P.L. tests, to about a third of its height at the generator position) and prevented from growing for a distance of the order of 15–20 generator heights downstream. In the regions BC, the height to which the de-energized air is swept increases at first and the velocity contour $u/U_0 = 0{\cdot}95$ soon forms a narrow neck, $B'C'$. When this is a minimum, the thickness of the layer for which $u/U_0 < 0{\cdot}85$ is reasonably small across the whole span.

In the N.P.L. tests, the effects of generators on the separation upstream of a step were investigated; it was found that separation was delayed to a point downstream of its normal position in the regions AB but occurred earlier than normal in the regions BC, where the resultant velocity near the surface is outwards. Nevertheless, for good generator designs the pressure recovery at the upstream edge of the step was increased in both regions.

Two arrangements of generators have so far been considered, see Fig. 43a and b. The counter-rotating arrangement has usually been found the more effective in diffusers or on straight wings, but the co-rotating one is sometimes the better on sweptback wings because vortices downstream of co-rotating blades flow in a direction at an angle to the stream direction and can be used to oppose the outflow of the boundary layer and so to augment the other favourable effects of the generators[38]. Tanner has now introduced an arrangement to produce counter-rotating vortices in alternate pairs – the 'biplane' arrangements sketched in Fig. 43c.

The N.P.L. tests have so far been of a preliminary nature, but have given some confirmation of Taylor's conclusions on optimum blade height and on the importance of location relative to the separation point. In conjunction with Taylor's results they enable a rational basis for the design of generator arrangements to be formulated tentatively. It is hoped to establish this by extending the low speed tests and by checking that the same design basis holds for eliminating or reducing shock-induced separation. Some preliminary observations have already been made at high speeds and apparatus is now ready for examining the effects and design of generators on a curved bump on the wall of the 9 in. × 3 in. wind tunnel.

---

*Low speed tunnel tests of vortex generators on sweptback wings have shown in one instance a marked improvement in pitching-moment characteristics[38], and in another only a small improvement in $C_{L\,max}$[39] but the generators were actually under the separated flow near the stall for this experiment.

**i.e. set so as to produce trailing vortices rotating in opposite directions.

One set of counter-rotating generators designed on the tentative basis to have $S/h = 3$, $c/h = 3$, $\alpha = 17$ deg, where h is blade height, c the blade chord, α the blade incidence and S the spacing between blades, has been tested on a 10 per cent thick RAE 102 section in the 20 in. × 8 in. high speed tunnel. Significant improvements were observed for the aerofoil at 2 deg incidence, Fig. 44, sufficient to eliminate most of the trough from the C_L vs. M curve and to allow the centre of pressure to move much more smoothly to its 'supersonic' position. Some of the data obtained from pressure plotting and flow photography in this experiment are presented in Figs. 45, 46 and 47. The generators delayed the occurrence of separation from about $M_0 = 0{\cdot}775$ to $M_0 = 0{\cdot}805$, Fig. 45a. The rearward movement of the upper-surface shock continued correspondingly further before the characteristic slowing up occurred, Fig. 45b. The delay in separation corresponded to an increase in the local Mach number, M_1, just upstream of of the shock from 1·26 to 1·37, Fig. 45c. The value of M_1 later fell slightly, to 1·36 at $M_0 = 0{\cdot}85$ but the boundary layer still separated at the foot of the shook, probably because the delay in the separation had been sufficient to allow the shock to move back out of the region where the generators would be most effective (about 16 generator heights downstream from the generators, or at about 0·55 chord).

That the separation when it occurred was much less severe than for the plain aerofoil can be seen from the pressure distributions and schlieren photographs for $M_0 = 0{\cdot}83$ in Figs. 46 and 47 respectively. The pressure rise through the upper surface shock was slightly greater with vortex generators and the rate of recovery downstream of the shock considerably greater. The total pressure recovery would have been much larger with generators than without if the upper-surface shock had not moved rearwards. This 'apparent' increase in recovery is the change which had to be accommodated in establishing equality of pressure at the trailing edge for the new conditions, and was achieved by (i) a rearward movement of the upper-surface shock to reduce the 'apparent' increase to a relatively small real one and (ii) a small forward movement of the lower-surface shock to give this same 'real' increase.

The upper-surface pressure distribution shows the extent of the local disturbance near the generators and illustrates a difficulty that is encountered in testing vortex generators at low Reynolds numbers on small models, where the obstruction to the flow is relatively large for two reasons. The ratio of blade height to aerofoil chord is larger than for high Reynolds numbers, and it is also difficult to reduce the thickness of the blades in proportion to the model scale.

The schlieren photograph with generators, Fig. 47a shows the local disturbance at the generator and also shows what appears to be a wide band of turbulent flow originating at the generators and persisting to the trailing-edge. This must be the de-energized air which is swept away from the surface in the regions corresponding to BC in Fig. 42. The comparatively thin boundary layer remains attached to the surface up to the foot of the shock where it can be seen to separate. The dead-air region is small compared with that for no generators.

A very much smaller effect was produced by these same generators on the lift due to 4 deg deflection of the 0·25 chord flap (zero aerofoil incidence), Fig. 48. This is because the expansion at the hinge of the flap, on the upper surface, gives rise to a local Mach number of about 1·45[41] and therefore a more severe separation. The proportion of the small increase in lift is very much the same as that in aileron effectiveness produced by vortex generators on the F–86A (Sabre) aircraft[11] (Fig. 21).

Pressure distributions for the upper surface of the D–558–I aircraft in flight [36]. Fig. 49, show effects from vortex generators qualitatively the same as those observed on the RAE 102 aerofoil (Fig. 46). The results for the F–86A (Sabre) aircraft, that even after separation occurred in the presence of vortex generators certain of its effects were less severe, (notably the aileron floating angles (Fig. 28) and the intensity of buffeting[11]), are qualitatively in agreement with the aerofoil results.

It seems reasonable to suppose that ordinary counter-rotating generators better located would have eliminated separation for the 10 per cent RAE 102 aerofoil at 2 deg incidence, and that there is therefore a fairly wide field of application in which such arrangements would be effective. The problems of the loss of effectiveness of flap-type controls and separation at higher C_L's are however more difficult because of the higher local Mach numbers and stronger shock waves involved. Further improvements in the

effectiveness of vortex generators should, however, be fairly easily obtained by using tandem rows or biplane arrangements. These will be tried in the experiment in the N.P.L. 9 in. × 3 in. wind tunnel. The use of blades of aerofoil section instead of thin flat plates or tapered blades might also give greater effectiveness.

Schemes for generating vortices near the boundary layer other than by blades normal to the surface have been suggested and some will be investigated at the N.P.L., initially at low speeds. Small wedge-shaped bodies have already been tried in the U.S.A. and Australia.

5.5. *Fences.*

Fences have frequently been used to improve the behaviour of sweptback wings, particularly in those speed ranges where the flow breaks down from the leading edge. They are often quite effective also in reducing the effects of shock-induced separation as is illustrated by the way in which the 'pitch-up' was delayed on the F–86A (Sabre) aircraft[11] (Fig. 25b). A small improvement due to one fence on the D–558–II aircraft has also been recorded[21]. Further examples are given in Ref. 31.

Fences have often been thought of as a means of obstructing the outward drift of boundary-layer air. Küchemann[32] has pointed out, however, that they have other effects at low speeds. He shows for example that they can be used as 'reflection plates' to give a more uniform spanwise loading or to delay the formation of 'part-span' vortex sheets and 'to slow their movements down in a desirable manner'. The mechanism by which they reduce the effects of shock-induced separation when it occurs well downstream of the leading edge is not so well understood, but work is being done on the problem at the R.A.E.

An interesting and illustrative example, although for transition free at a fairly low Reynolds number, is quoted from NACA tests[42] on a twisted and cambered wing with 40 deg. sweepback and aspect ratio of 10. The fences extended forwards from the trailing edge rather than backwards from the leading edge as is more usual. Suitable arrangement of these was found to delay appreciably the unstable break in pitching moment for $M_0 = 0{\cdot}90$ (Fig. 50b). The pressure distributions (Fig. 50a) and approximate areas of separation (Fig. 50c) for $\alpha = 6$ deg show how the separation was more severe outboard of about 0·4 semispan than inboard. The amount of flow separation was reduced by the fences, and was eliminated in parts of the span just outboard of the fences. An understanding of the mechanism which produced this change might lead to developments in the applications of such fences to wings of lower aspect ratio. They might, for example, help to prevent separation from occurring on ailerons or all-moving wing-tips if placed just inboard of these control surfaces. Like vortex generators they can be used on current aircraft relatively easily. The absence of separation outboard of the fences might be related to its frequent absence from root sections near a fuselage. It might be associated with some re-distribution in the spanwise loading and reduction of local Mach numbers, but this is not supported by the approximate isobars shown in Ref. 42. The most plausible explanation is probably that given in Ref. 42, namely, that spanwise flow of air occurs over the forward part of the fence and sets up some vortex action which has an effect downstream similar to that of the trailing vortices behind vortex generators. This is supported by the pressure distributions on this wing at low speeds, $\alpha = 18$ deg, at a station just outboard of a fence position, Fig. 51. In the absence of the fence the flow was separated and the pressure nearly constant over most of the chord, but the fence gave a small low pressure region near its own leading edge and considerable pressure recovery between there and the trailing edge.

5.6. *Leading-edge Devices.*

Extensions and other modifications to the leading edges of sweptback wings have been used to improve their pitching moment variations and performance[31]. No explanation of how their mechanism is associated with a reduction in the effects of shock-induced separation is known to the authors, but it seems likely that if an association could be established it would lead to further developments of these devices.

6. *Conclusions and Suggestions for Further Work.*

It is shown that the form of the variation with free-stream Mach number of the trailing-edge pressure coefficient $C_{pT.E.}$ for straight and swept wings is the same as for two-dimensional aerofoils. When a certain free-stream Mach number is reached, $C_{pT.E.}$ begins to diverge rapidly from the smooth and gradual variation which occurs at lower Mach numbers, and there are strong reasons for supposing that this arises from the onset of boundary-layer separation at the shock wave on the upper surface. Using this criterion to detect separation, it is found from flight-test results that separation occurs on straight wings for approximately the same value of the local Mach number M_1 just ahead of the shock as for two-dimensional aerofoils with turbulent boundary layers. For swept wings an attempt is made to compare the component normal to the shock of the local Mach number just upstream with the value of M_1 observed on aerofoils, but difficulties arise from the absence of data on the shape of the shock and the flow direction immediately upstream. The few comparisons which have been made suggest that there is reasonable agreement near the middle of the span, but not near the root or tip. In the cases examined, separation occurred earlier on the outboard sections than near the root.

For straight wings it is found that a number of changes in the aerodynamic characteristics are associated with the onset of separation at the shock wave. These are due mainly to the effects of separation on the rates of movement of the shock waves with change of Mach number, and are qualitatively similar to those observed on two-dimensional aerofoils. Examples are given of undesirable effects which have been encountered on several aircraft and which are shown to be associated with boundary-layer separation. These include wing dropping which has been reported for both straight and swept-wing aircraft, and the 'pitch-up' instability which is peculiar to swept-back wings.

When the flow at the trailing edge becomes supersonic, the conditions on the two surfaces become independent, and separation then has a much smaller effect on the differential movement of the shock waves and hence on the overall loading. The sweep of the trailing edge is thus an important parameter so far as the effects of shock-induced separation in transonic flow are concerned, and there are advantages in an unswept trailing edge.

In an attempt to obtain a clearer understanding of the mechanism which leads to high-speed buffeting, a review is given of N.A.C.A. wind-tunnel measurements of the pressure fluctuations at the surfaces of aerofoils and in their wakes. These observations show that large fluctuations may occur under the conditions for which separation would be expected; a detailed correlation with the onset of separation is not possible because the data required are not available. A comparison is made between the flight-determined buffet boundaries of several aircraft and the conditions for separation as determined from measurements of the pressure at the trailing edge. There is reasonable agreement for straight wings but for swept wings a detailed comparison is not possible because of the absence of pressure measurements.

Although it is fairly well established that many of the undesirable characteristics of high-speed aircraft are associated with the onset of boundary-layer separation at shock waves, in many cases a more detailed correlation is desirable than is possible on the basis of the existing data. There is, therefore, a need for further experimental work especially on swept wings. This work should, if possible, include observations of the shape of the shock wave near the surface, and of the local flow direction upstream so that a comparison can be made with the results of experiments on two-dimensional aerofoils and fundamental investigations of the interaction between shock waves and boundary layers. It would be of value to make detailed wind-tunnel observations (including measurements of fluctuations of pressure and downwash) of the flow round a model of the swept wing of a modern high-speed aircraft, and to compare them with the results of flight tests.* This proposal, and suggestions for experiments of a more fundamental character are under consideration. An indication of the conditions under which separation occurs at high speeds would be very useful in all experiments on both straight and swept wings, and it is possible that this can be achieved most simply by measuring the pressure near the trailing edge.

Considerable effort is being devoted to the study of devices which can be used on the wings of existing aircraft to eliminate or minimize the adverse effects of separation now being encountered in transonic flight. Vortex generators have been found to delay the onset of separation and to reduce its severity on

*The tunnel tests should, of course, be made with transition fixed in order to ensure a valid comparison.

aerofoils and also in flight where distinct improvements have been observed in the behaviour of certain aircraft. It should be possible to increase the effectiveness of vortex generators and hence to delay separation still further by improving their design and finding the optimum chordwise location. Some work on these aspects is in hand.

Improvements have been observed from the use of fences even when the separation occurs some way downstream of the leading edge. It seems likely that they do more than prevent the spanwise flow of boundary-layer air and if this is so, an understanding of the fundamental mechanism might lead to further applications.

Boundary-layer suction has been used successfully to increase the pressure recovery downstream of a shock wave in a nozzle by suppressing separation. Similar increases in pressure recovery would lead to considerable improvements in many of the adverse effects of separation described in earlier parts of this report and in Ref. 1. Further work should be done on the application of suction to aerofoils and wings, and the use of blowing, particularly for flap-type controls, should also be considered.

Leading-edge extensions and other leading-edge devices have been shown to delay the adverse effects of separation. It is suggested that their mechanism should be studied with a view to possible developments.

Although very few data are available for sections and wings with turbulent boundary layers, they are probably sufficient to enable the section and planform to be designed so that separation is either absent or has negligible effects at low angles of incidence. The high local Mach numbers which lead to separation are still likely to occur for high incidences or control deflections, however, and interest will, therefore, probably continue in devices for eliminating separation or for alleviating its effects under these conditions. It is under these conditions of high incidence or control deflection that reliable section and wing data are, perhaps, most urgently required.

LIST OF SYMBOLS

b	Span
c	Chord
t	Wing thickness
x	Distance along the chord line from the leading edge
x_s	Value of x at the shock wave
y	Spanwise distance, or distance perpendicular to the free-stream direction (Fig. 31), or perpendicular to the chord line (Fig. 41)
A	Aspect ratio
λ	Taper ratio
α	Angle of incidence
β	Angle of sideslip
ε	Downwash angle
η	Elevator angle
ξ	Aileron angle
u	Local velocity
U_0	Free-stream velocity
$\frac{1}{2}\rho_0 U_0^2$	Free-stream dynamic pressure
M	Local Mach number just outside the boundary layer
M_0	Free-stream Mach number
M_1	Value of M just ahead of the shock
M'	Local Mach number within the boundary layer
R	Reynolds number based on chord
p	Local static pressure
p_0	Free-stream static pressure
H	Local total head
H_0	Free-stream total head

Δ_p	Amplitude of the static-pressure fluctuations at the surface
Δ_H	Amplitude of the total-head fluctuations in the wake
C_p	Pressure coefficient $\frac{p-p_0}{\frac{1}{2}\rho_0 U_0^2}$
$C_{pT.E.}$	Value of C_p at the trailing edge
C_L	Lift coefficient
C_l	Rolling moment coefficient
C_N	Normal-force coefficient for the wing
C_{N_A}	Normal-force coefficient for the complete aircraft
C_n	Normal-force coefficient for the wing section
C_m	Pitching-moment coefficient
$\frac{pb}{2V\xi}$	Measure of the effectiveness of an aileron control

REFERENCES

No.	*Author(s)*	*Title, etc.*
1	D. W. Holder, H. H. Pearcey and G. E. Gadd	The interaction between shock waves and boundary layers.
	J. Seddon	With a note on the effect of the interaction on the performance of supersonic intakes. A.R.C. C.P. 180. February 1954.
2	D. E. Beeler, ... M. D. McLaughlin and D. C. Clift	Measurements of the chordwise pressure distributions over the wing of the XS–1 research airplane in flight. NACA RM L8G21. 1948.
3	H. A. Carner and .. .. R. J. Knapp	Flight measurements of the pressure distribution on the wing of the X–1 airplane (10 per cent thick wing) over a chordwise station near the midspan in level flight at Mach numbers from 0·79 to 1·00 and in a pull-up at a Mach number of 0·96. NACA RM L50H04. 1950.
4	R. J. Knapp and .. .. G. V. Wilken	Tabulated pressure coefficients and aerodynamic characteristics measured on the wing of the Bell X–1 airplane in pull-ups at Mach numbers from 0·53 to 0·99. NACA RM L50H28. November, 1950.
5	H. A. Carner and .. .. M. M. Payne	Tabulated pressure coefficients and aerodynamic characteristics measured on the wing of the Bell X–1 airplane in level flight at Mach numbers from 0·79 to 1·00 and in a pull-up at Mach number of 0·96. NACA RM L50H25. September, 1950.
6	L. A. Smith	Tabulated pressure coefficients and aerodynamic characteristics measured on the wing of the Bell X–1 airplane in an unaccelerated stall and in pull-ups at Mach numbers 0·74, 0·75, 0·94 and 0·97. NACA RM L51B23. June, 1951.
7	E. R. Keener and M. Pierce	Tabulated pressure coefficients and aerodynamic characteristics measured in flight on the wing of the Douglas D–558–I airplane for a 1*g* stall, a speed run to a Mach number of 0·90 and a wind-up turn at a Mach number of 0·86. NACA RM L50J10. December, 1950.
8	E. R. Keener and .. .. R. M. Bandish	Tabulated pressure coefficients and aerodynamic characteristics measured in flight on the wing of the D–558–I research airplane through a Mach number range of 0·80 to 0·89 and through a normal-force coefficient range at Mach numbers of 0·61, 0·70, 0·855 and 0·88. NACA RM L51F12. August, 1951.
9	E. R. Keener and .. .. J. R. Peele	Tabulated pressure coefficients and aerodynamic characteristics measured in flight on the wing of the Douglas D–558–I airplane throughout the normal-force coefficient range at Mach numbers of 0·67, 0·74, 0·78 and 0·82. NACA RM L50L12a. January, 1951.

REFERENCES—*continued*

No.	*Author(s)*	*Title, etc.*
10	J. R. Collingbourne and A. C. S. Pindar ..	Balance and pressure measurements at high subsonic speeds on model of a swept-wing aircraft (Hawker E38/46–P.1052) and some comparisons with flight data. A.R.C. R. & M. 3165. February 1953.
11	N. M. McFadden, G. A. Rathert, Jr. and R. S. Bray	The effectiveness of wing vortex generators in improving the maneuvering characteristics of a swept-wing airplane at transonic speeds. NACA RM A51J18. Superseded by T.N.3523. September, 1955.
12	L. J. Lina and W. H. Reed III	A preliminary flight investigation of the effects of vortex generators on separation due to shock. NACA RM L50J02. November, 1950.
13	B. E. Tinling and A. E. Lopez	The effects of Reynolds number at Mach numbers up to 0·94 on the loading on a 35 deg swept-back wing having NACA 651A012 streamwise sections. NACA RM A52B20. June, 1952.
14	H. M. Drake	Measurements of aileron effectiveness on the Bell X–1 airplane at Mach numbers between 0·9 and 1·06. NACA RM L9G19a. August, 1949.
15	S. B. Anderson, E. A. Ernst and R. D. Van Dyke	Flight measurements of the wing-dropping tendency of a straight-wing jet airplane at high subsonic Mach numbers. NACA RM A51B28. April, 1951.
16	—	Private communication from the Royal Aircraft Establishment.
17	H. K. Strauss and E. M. Fields	Flight investigation of the effect of thickening the aileron trailing edge on control effectiveness for sweptback tapered wings having sharp- and round-nose sections. NACA RM L9L19. May, 1950.
see also		
	E. M. Fields and H. K. Strauss	Free-flight measurements at Mach numbers from 0·7 to 1·6 of of some effects of airfoil-thickness distribution and trailing-edge angle on aileron rolling effectiveness and drag for wings with 0 deg and 45 deg sweepback. NACA RM L51G27. October, 1951.
18	H. M. Drake, J. R. Carden and H. P. Clagett	Analysis of longitudinal stability and trim of the Bell X–1 airplane at a lift coefficient of 0·3 to Mach numbers near 1·05. NACA RM L51H01. October, 1951.
19	S. B. Anderson and R. S. Bray ..	A flight evaluation of the longitudinal stability characteristics associated with the pitch-up of a swept-wing airplane in maneuvering flight at transonic speeds. NACA RM A51I12. Superseded by R.1237. 1955.
20	G. A. Rathert, Jr., H. L. Ziff and G. E. Cooper	Preliminary flight investigation of the maneuvering accelerations and buffet boundary of a 35 deg swept-wing airplane at high altitude and transonic speeds. NACA RM A50L04. February, 1951.

REFERENCES—*continued*

No.	*Author(s)*	*Title, etc.*
21	J. Fischel and J. Nugent ..	Flight determination of the longitudinal stability in accelerated maneuvers at transonic speeds for the Douglas D–558–II research airplane including the effects of an outboard wing fence. NACA RM L53A16. May, 1953.
22	H. H. Pearcey and .. .. M. E. Faber	Detailed observations made at high incidences and at high subsonic Mach numbers on Goldstein 1442/1547 aerofoil. A.R.C. R. & M. 2849. November, 1950.
23	S. B. Anderson, E. A. Ernst and R. D. Van Dyke, Jr.	Flight measurements of the wing-dropping tendency of a straight-wing jet airplane at high subsonic Mach numbers. NACA RM A51B28. April, 1951.
24	D. G. Stone	Wing-dropping characteristics of some straight and swept wings at transonic speeds as determined with rocket-powered models. NACA RM L50C01. May, 1950.
25	A. Ferri	Preliminary investigation of downwash fluctuations of a high-aspect-ratio wing in the Langley 8 ft high-speed tunnel. NACA RM L6H28b. April, 1946.
26	M. D. Humphreys	Pressure pulsations on rigid airfoils at transonic speeds. NACA RM L51I12. December, 1951.
27	M. D. Humphreys and .. J. D. Kent	The effects of camber and leading-edge-flap deflection on the pressure pulsations on thin rigid airfoils at transonic speeds. NACA RM L52G22. October, 1952.
28	R. M. Sorenson, J. A. Wyss and J. C. Kyle	Preliminary investigation of the pressure fluctuations in the wakes of two-dimensional wings at low angles of attack. NACA RM A51G10. October, 1951.
29	B. N. Daley and R. S. Dick	Effect of thickness, camber, and thickness distribution on airfoil characteristics at Mach numbers up to 1·0. NACA RM L52G31a. Superseded by T.N.3607. March, 1952.
30	B. L. Gadeberg and .. H. L. Ziff	Flight-determined buffet boundaries of ten airplanes and comparisons with five buffeting criteria. NACA RM A50I27. January, 1951.
31	C. J. Donlan and J. Weil ..	Characteristics of swept wings at high speeds. NACA RM L52A15. 1952.
32	D. Küchemann	Types of flow on swept wings with special reference to free boundaries and vortex sheets. A.R.C. 15 756. March, 1953.
33	J. R. Sterrett, R. W. Dunning and M. J. Brevoort	The use of suction to prevent shock-induced separation in a nozzle. NACA RM L50K20. January, 1951.
34	M. R. Head	Proposal for the prevention of separation at transonic speeds. M.O.S. B.L.C.C. B109. 1953.

REFERENCES—*continued*

No.	*Author(s)*	*Title, etc.*
35	C. duP. Donaldson ..	Investigation of a simple device for preventing separation due to shock and boundary-layer interaction. NACA RM L50B02a. November, 1950.
36	D. E. Beeler, D. R. Bellman and J. H. Griffith	Flight determination of the effects of wing vortex generators on the aerodynamic characteristics of the Douglas D–558–I airplane. NACA RM L51A23. August, 1951.
37	G. Hieser	An investigation at transonic speeds of the effects of fences, drooped nose and vortex generators on the aerodynamic characteristics of a wing-fuselage combination having a 6 per cent thick 45 deg sweptback wing. NACA RM L53B04. March, 1953.
38	J. A. Weiberg and .. .. G. B. McCullough	Wind-tunnel investigation at low speed of a twisted and cambered wing swept back 63 deg with vortex generators and fences. NACA RM A52A17. March, 1952.
39	W. J. Bursnall	Experimental investigation of the effects of vortex generators on the maximum lift of a 6 per cent thick symmetrical circular arc airfoil section. NACA RM L52G24. October, 1952.
40	J. Seddon and L. Haverty ..	Experiments in subsonic and supersonic flow in side intakes with boundary layer control. Part II. Tests with vortex generators. Unpublished M.O.A. Report.
41	H. H. Pearcey, ... R. C. Pankhurst and R. F. Cash	High-speed tunnel tests on a 10 per cent thick R.A.E. 102 two-dimensional aerofoil with 25 per cent flap. Results at zero incidence with 4 per cent flap deflection. A.R.C. 15 176. September, 1952.
42	F. W. Boltz and .. .. H. H. Shibata	Pressure distribution at Mach numbers up to 0·90 on a cambered and twisted wing having 40 per cent of sweepback and an aspect ratio of 10, including the effects of fences. NACA RM A52K20. March, 1953.
43	H. M. Drake	Measurements of aileron effectiveness of Bell X–1 airplane up to a Mach number of 0·82. NACA RM L9D13. June, 1949.

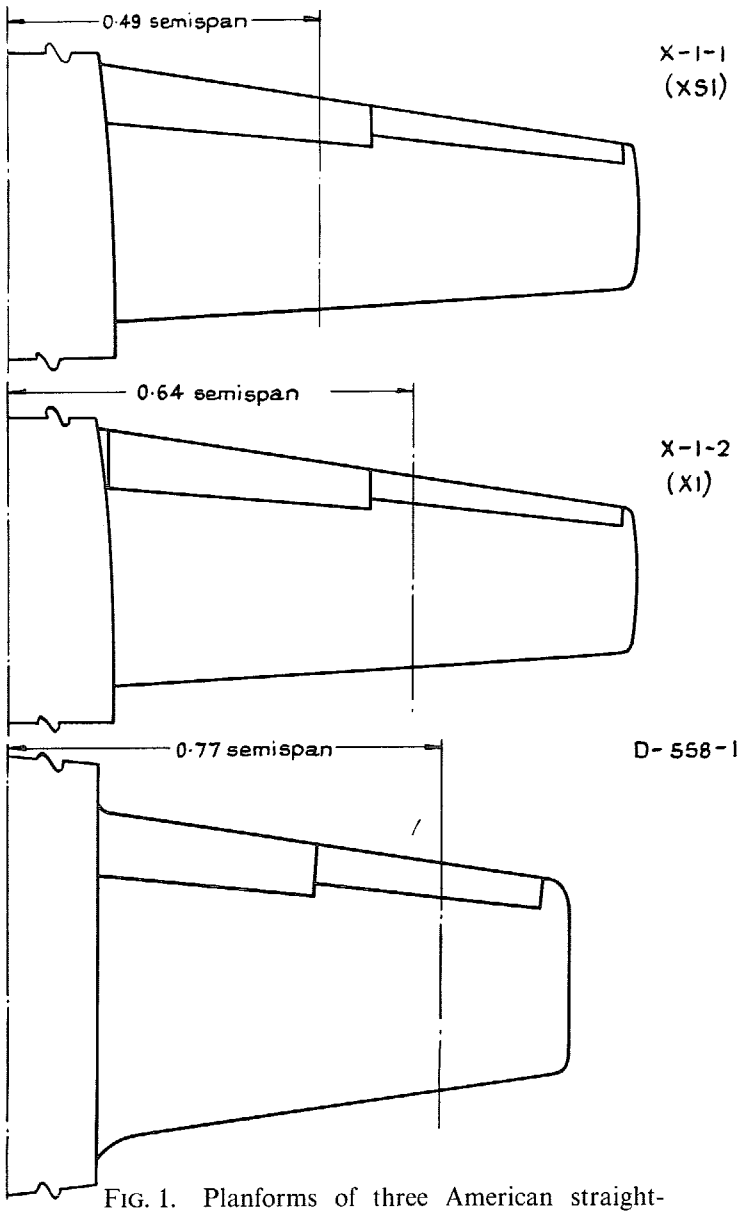

FIG. 1. Planforms of three American straight-wing aircraft showing the spanwise stations appropriate to the pressure plotting data used in succeed-

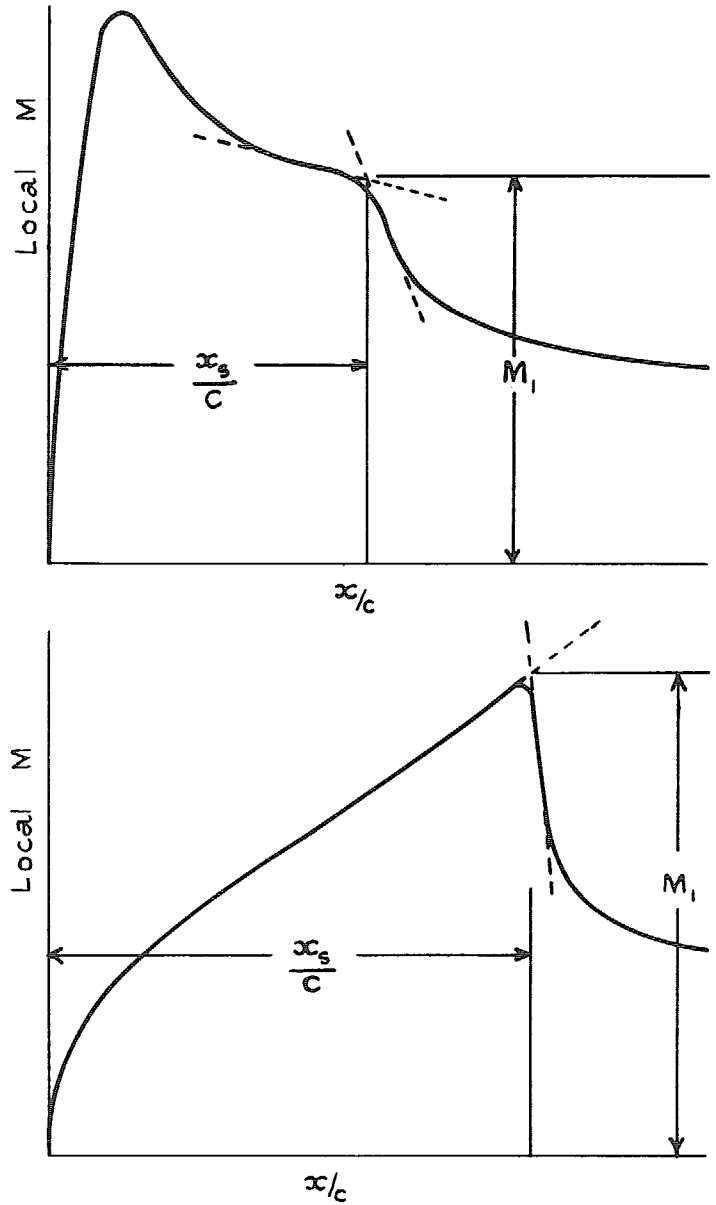

FIG. 2. Methods for defining the position x_s of the shock and the Mach number M_1 upstream

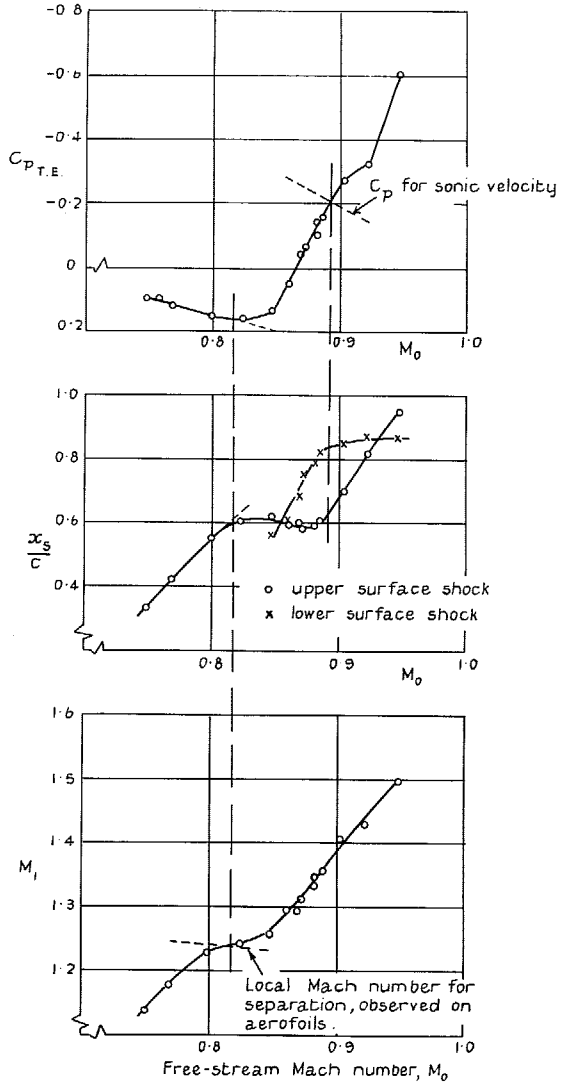

FIG. 3. Separation criteria and shock positions for the X–1–1 aircraft wing (Ref. 2) $C_{N_A} = 0{\cdot}33 \pm 0{\cdot}09$, $2y/b = 0{\cdot}49$.

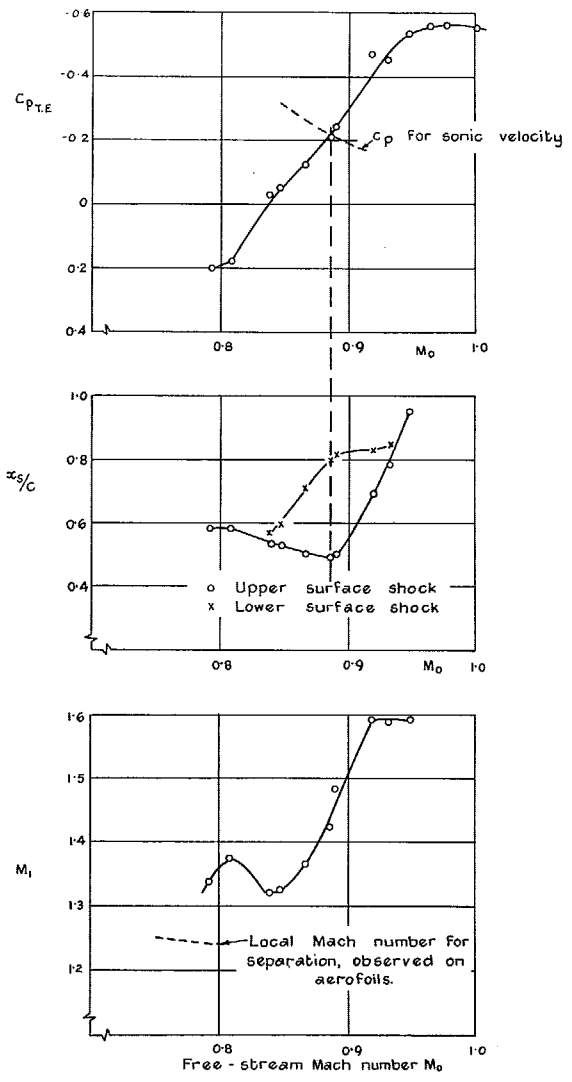

FIG. 4. Separation criteria and shock positions for the X–1–2 aircraft wing (Refs. 3 & 5) $C_{N_A} = 0{\cdot}3 \pm 0{\cdot}03$, $C_n = 0{\cdot}32 \pm 0{\cdot}08$, $\frac{2y}{b} = 0{\cdot}64$.

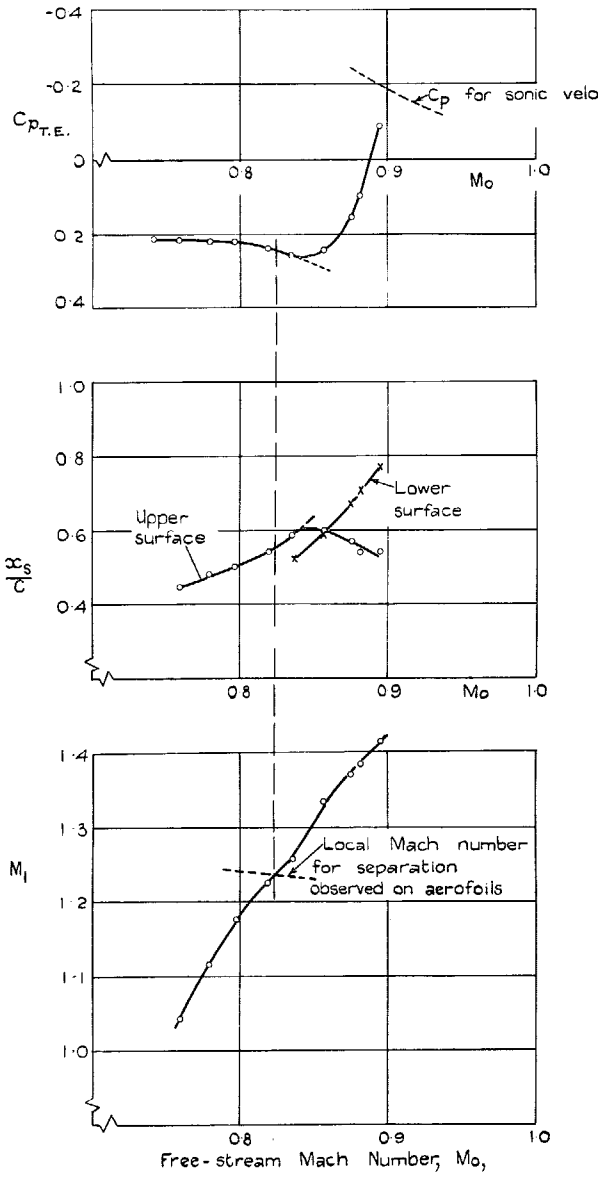

FIG. 5. Separation criteria and shock positions for the D–558–1 aircraft wing (Ref. 7) $C_{N_A} = 0{\cdot}25 \pm 0{\cdot}02$, $C_{l_\alpha} = 0{\cdot}25 - 0{\cdot}05\,\frac{2y}{b} = 0{\cdot}77$.

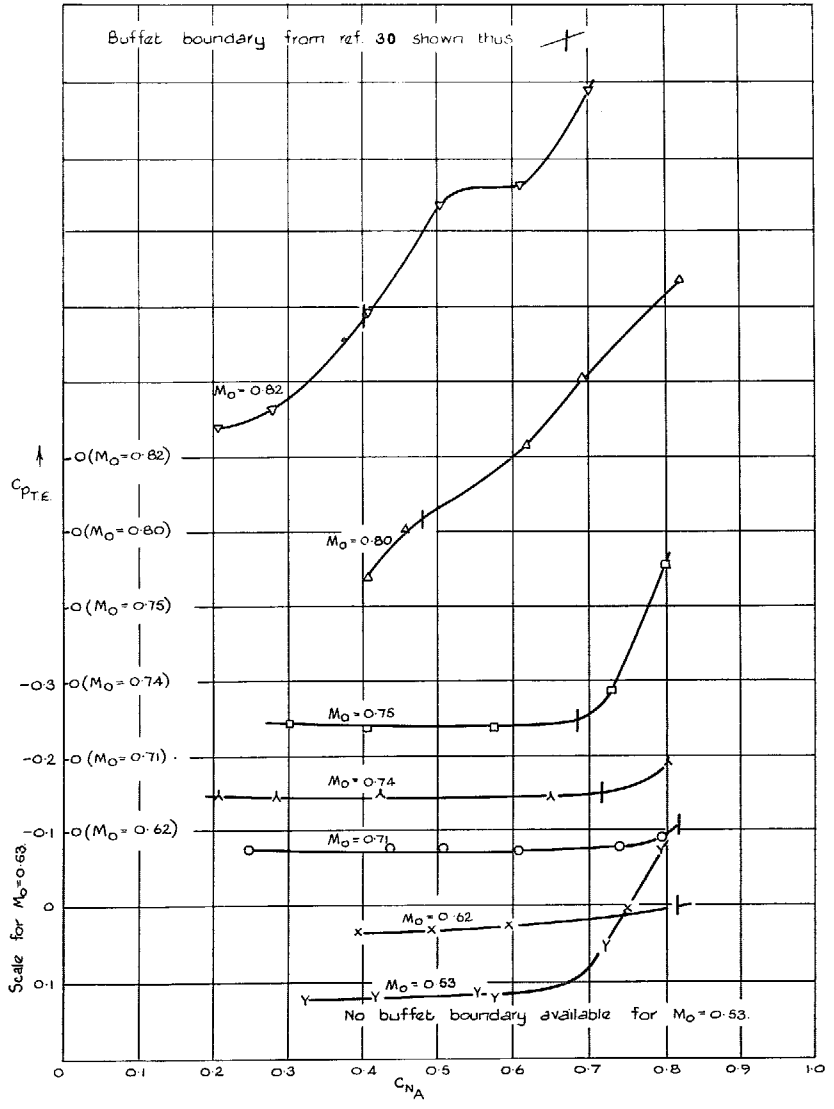

FIG. 6. Variation with C_{N_A} of the trailing-edge pressure coefficient for the X–1–2 aircraft wing. $\frac{2y}{b} = 0{\cdot}64$ (Refs. 4 and 6).

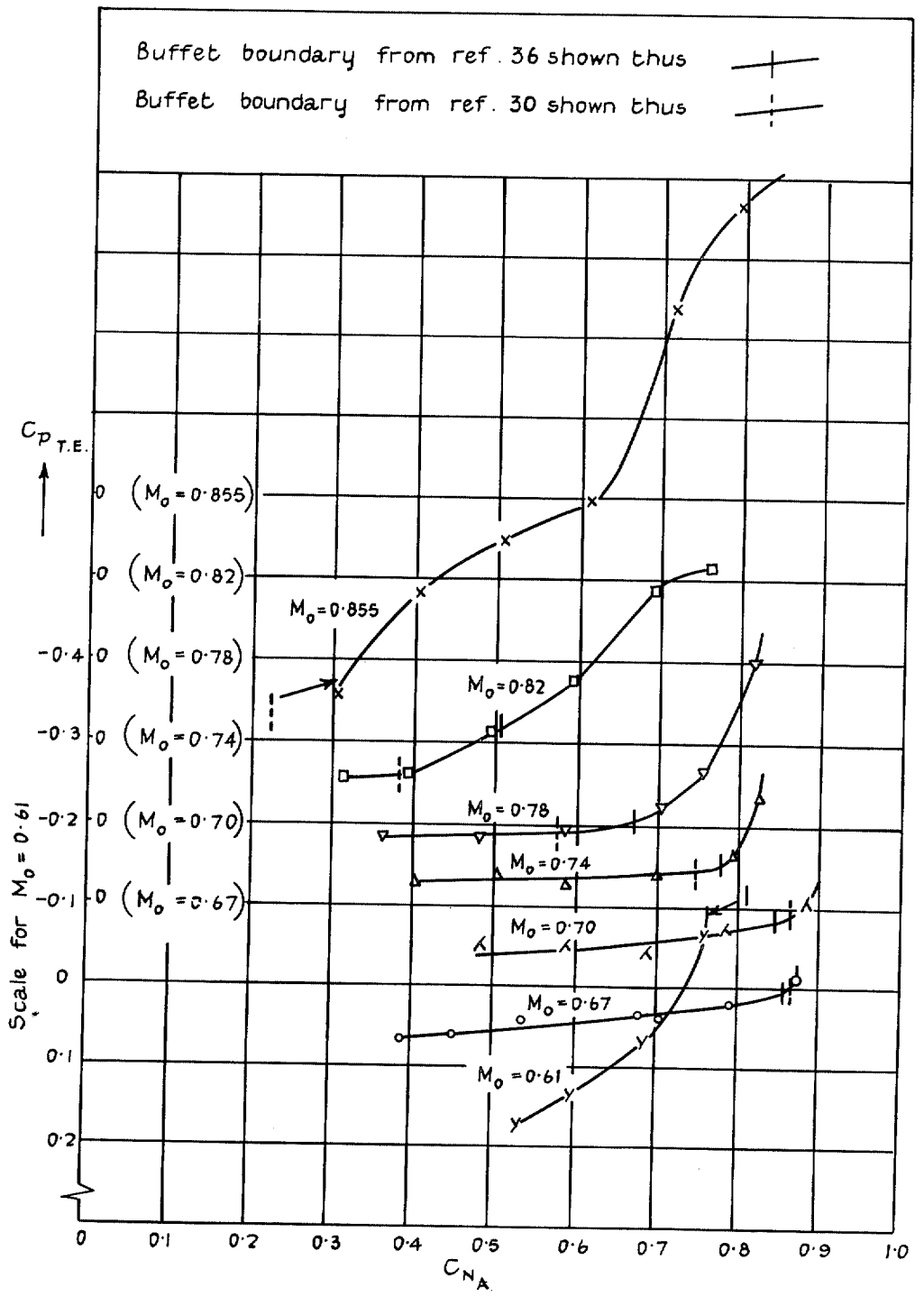

FIG. 7. Variation with C_{N_A} of the trailing-edge pressure coefficient for the D–558–1 aircraft wing. $2y/b = 0.77$ (Refs. 8 and 9).

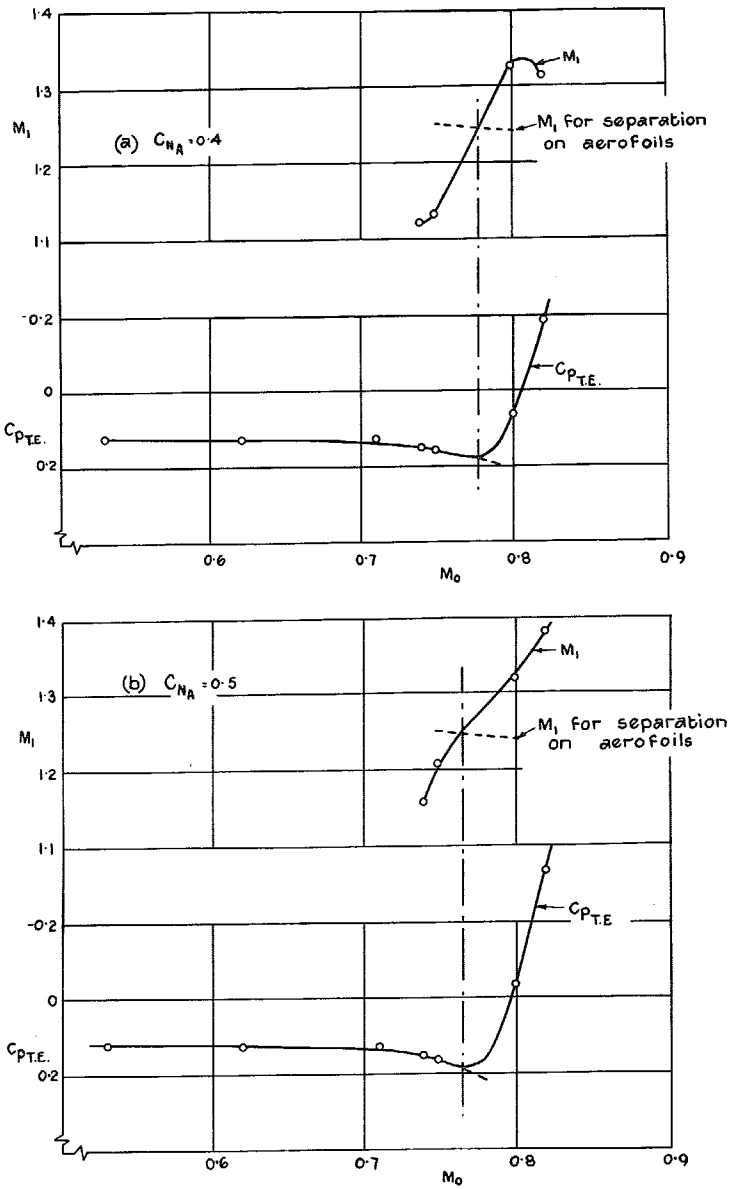

FIGS. 8a & b. Correlation between the divergence of $C_{pT.E.}$ for the X–1–2 aircraft wing and the M_1 criterion for separation on aerofoils.

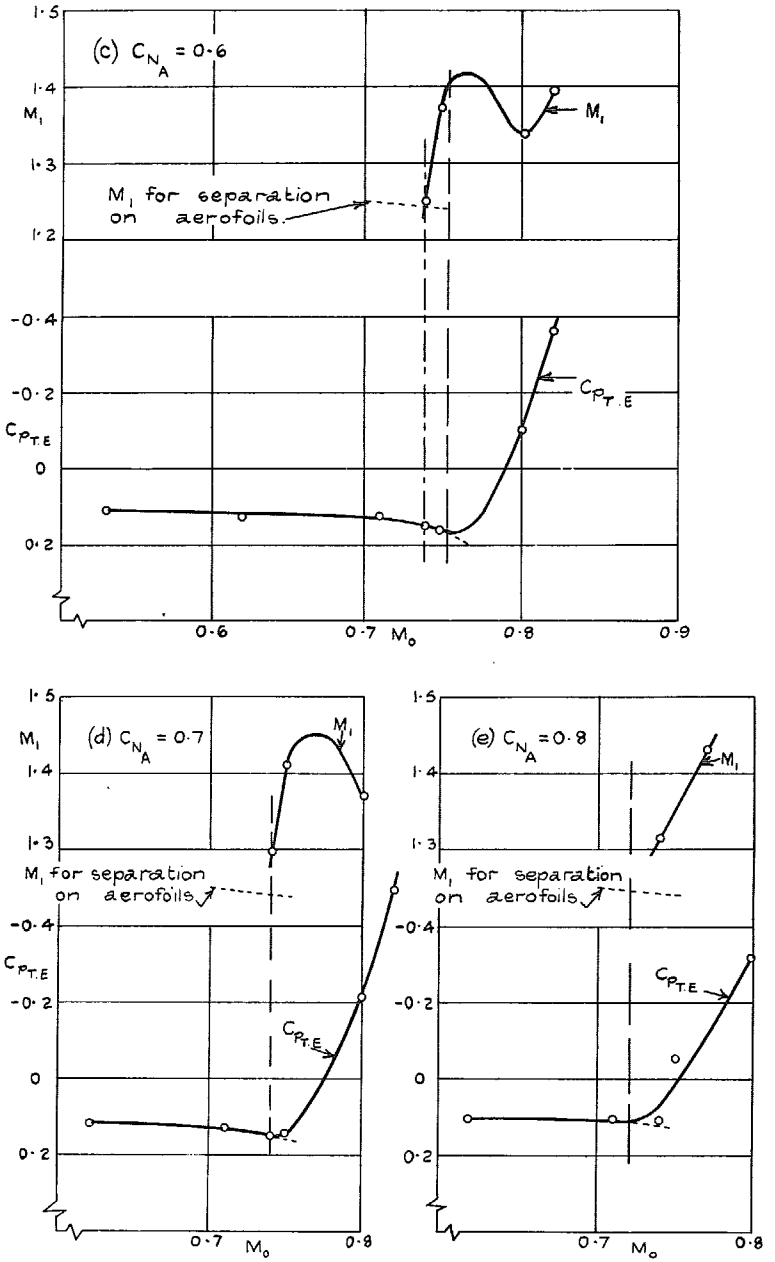

FIGS. 8c to e. Correlation between the divergence

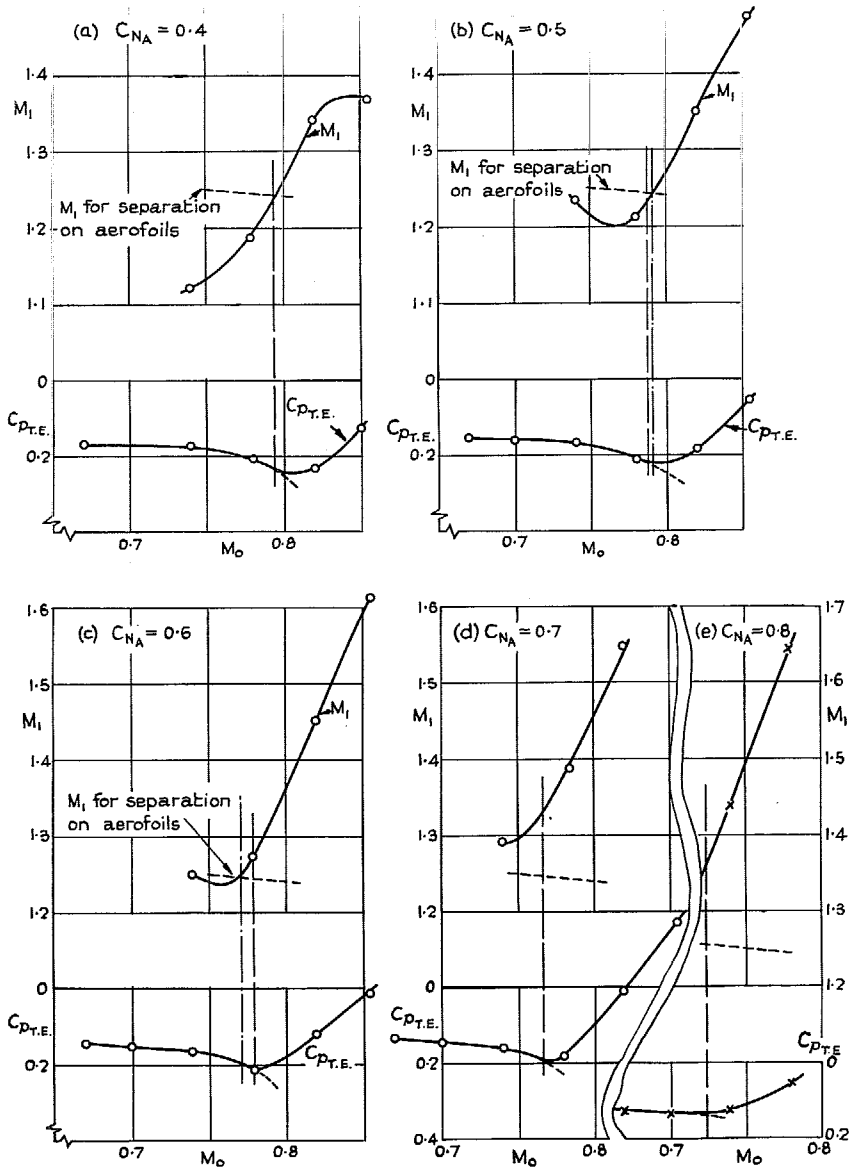

FIG. 9a to e. Correlation between the divergence of $C_{p_{T.E.}}$ for the D–558–I aircraft and the M_1 criterion for separation on aerofoils.

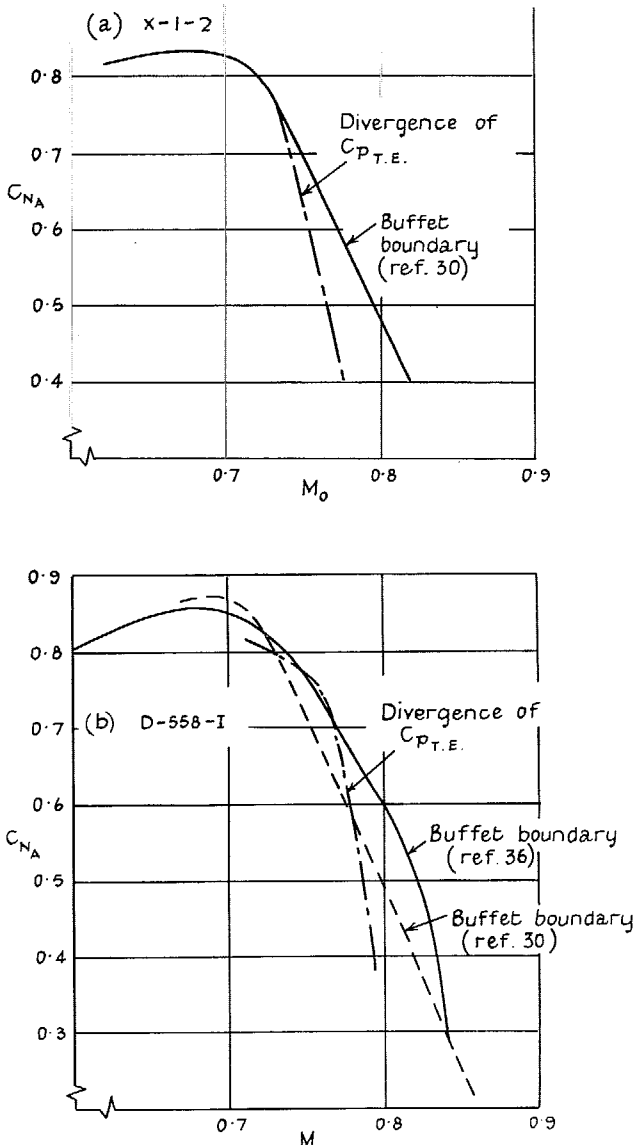

FIG. 10. Correlation between the divergence of the trailing-edge pressure coefficient and the buffet boundary.

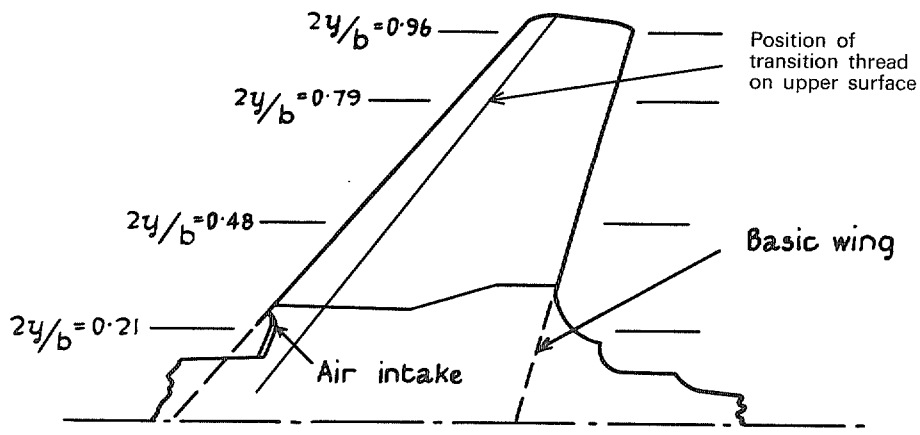

FIG. 11. Planform of the Hawker P1052 wing showing pressure-plotting stations used in R.A.E. tunnel tests (Ref. 10).

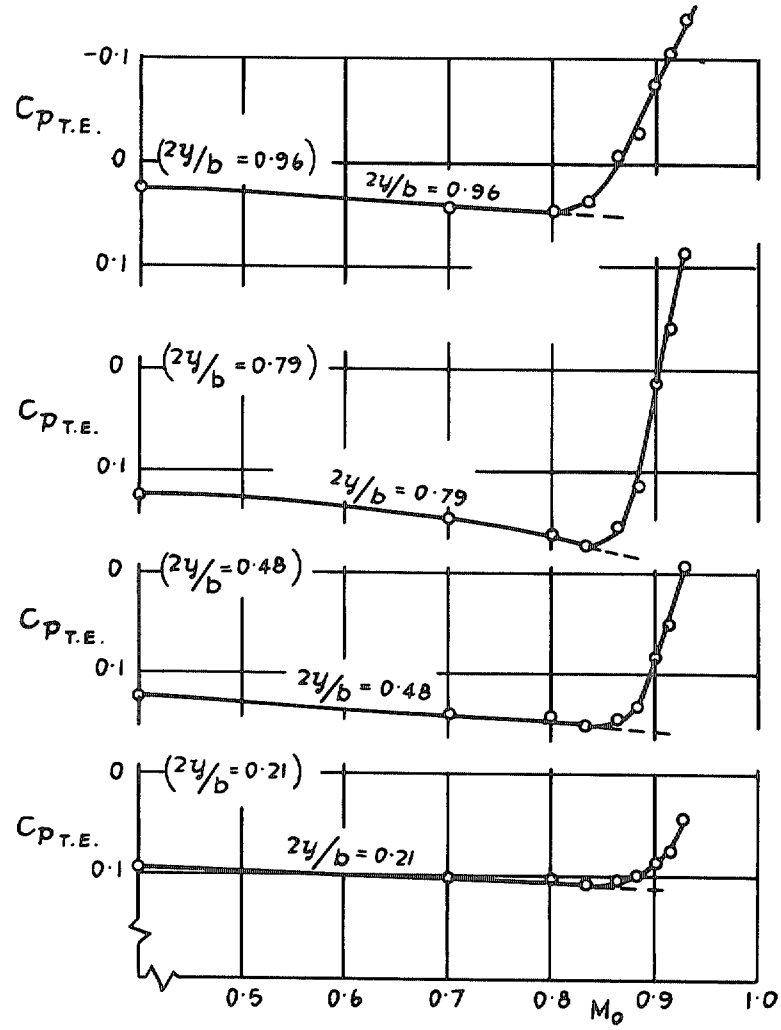

FIG. 12. Variation of $C_{p_{T.E.}}$ at four stations on the Hawker P1052 wing: $\alpha = 3$ deg (Ref. 10).

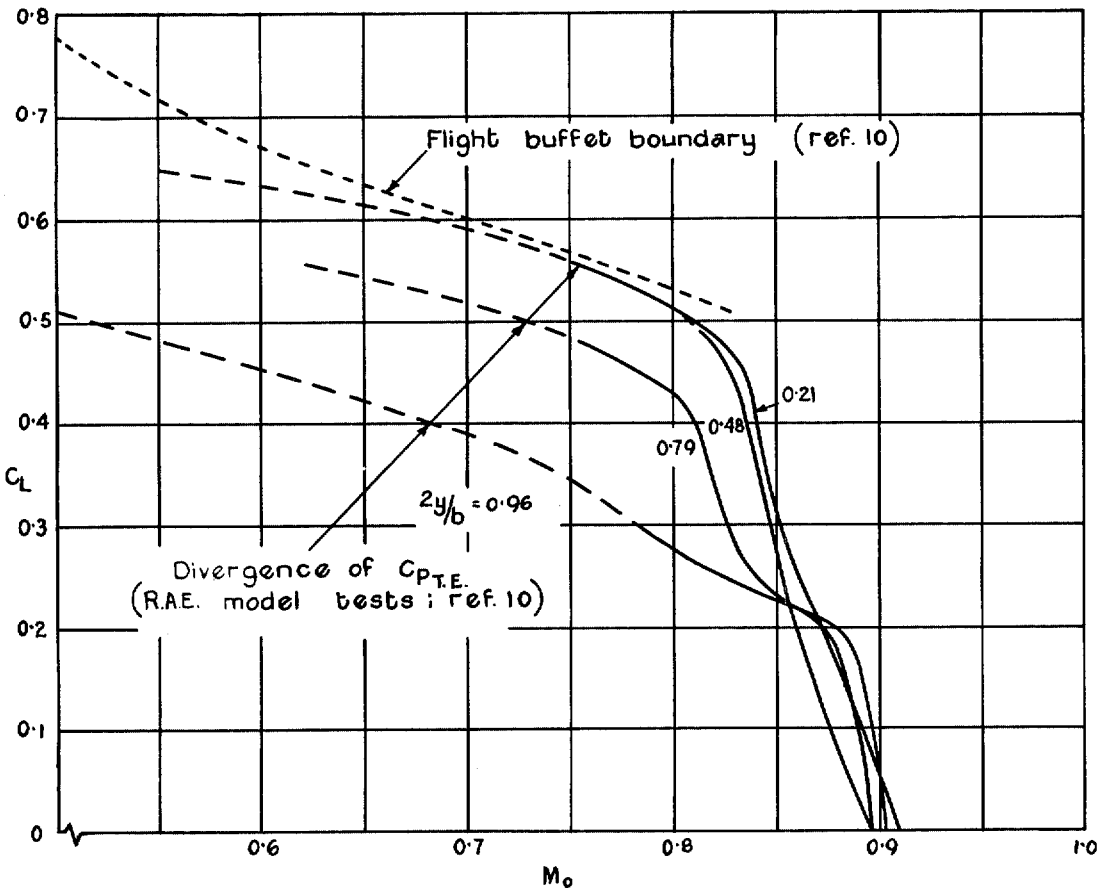

FIG. 13. Divergence of $C_{p_{T.E.}}$ at four stations on the Hawker P1052 wing, and buffet boundary.

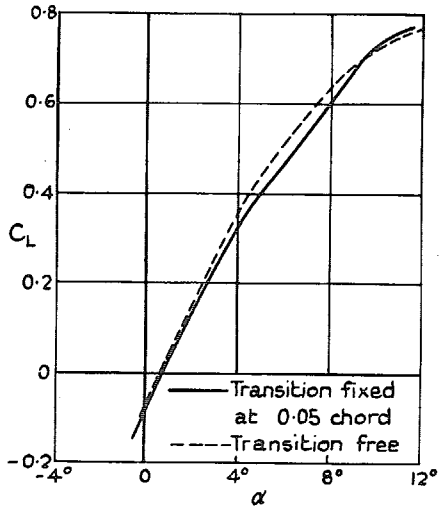

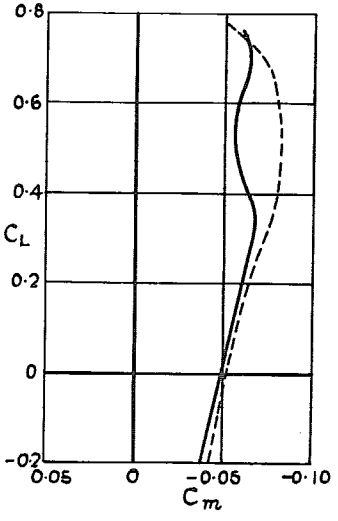

(a) Variation of C_L with α and of C_m with C_L (transition fixed and free).

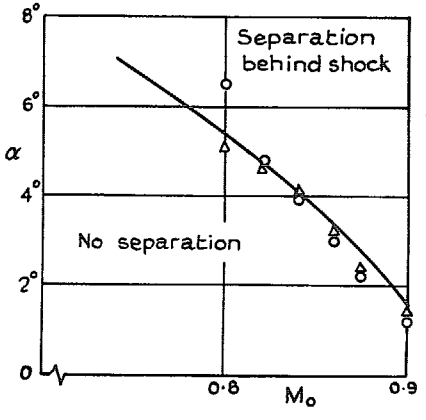

Separation boundary (from oil and tufts).

o Change in slope of C_L – α curves.

Δ Change in slope C_m – C_L curves.

(b) Occurrence of separation and correlation with change in $\frac{\partial C_L}{\partial \alpha}$ and $\frac{\partial C_m}{\partial C_L}$ (transition fixed).

FIG. 14a & b. Results for the Vickers Type 1000 wing; $M_0 = 0{\cdot}84$ (tunnel tests).

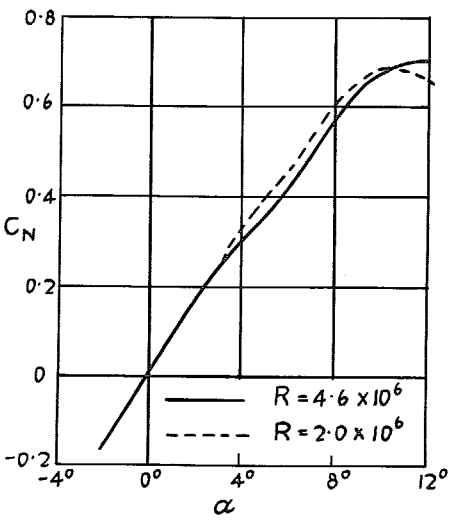

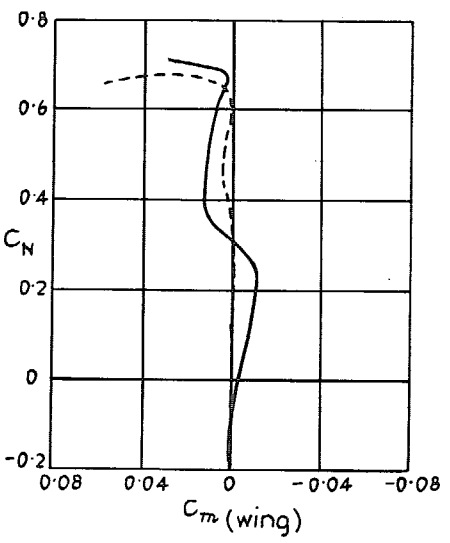

(a) Variation of C_N with α and of C_m with C_N; $M_0 = 0{\cdot}85$ ($R = 4{\cdot}6 \times 10^6$ and $2{\cdot}0 \times 10^6$)

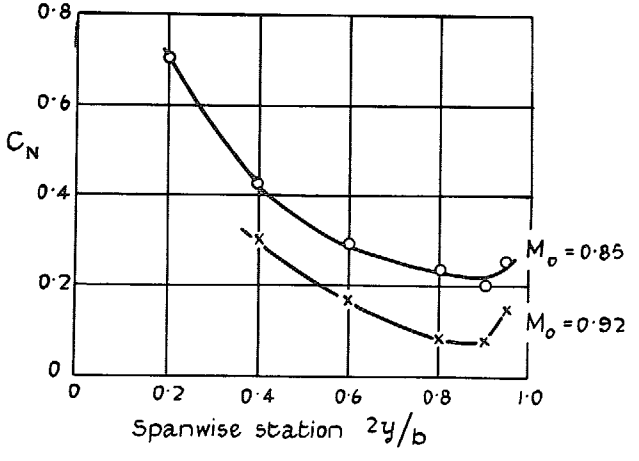

(b) Wing C_N for change in section $\frac{\partial C_n}{\partial \alpha}$, variation with spanwise position ($R = 4{\cdot}6 \times 10^6$)

FIG. 15a & b. Results for NACA 35 aerofoil

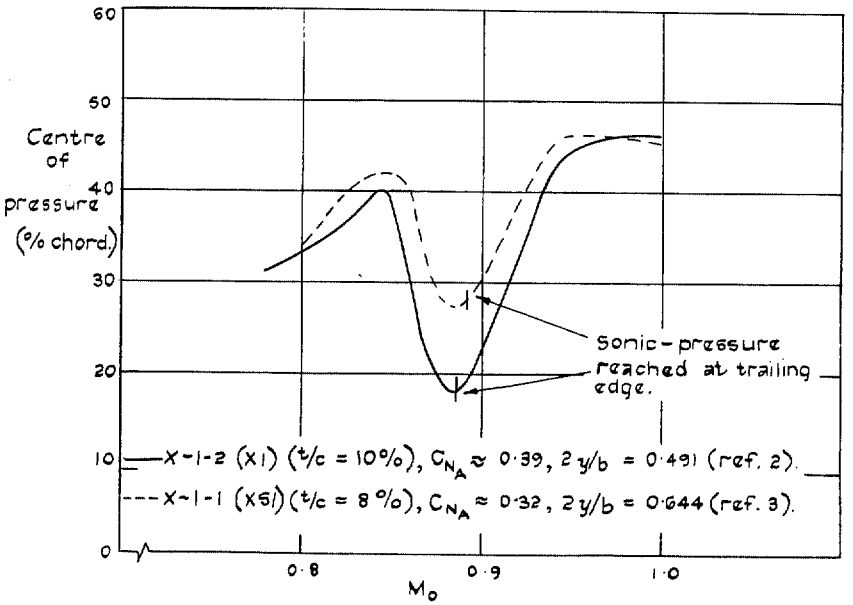

FIG. 16. Variation of section centre-of-pressure with Mach number for the X–1–1 and X–1–2 aircraft.

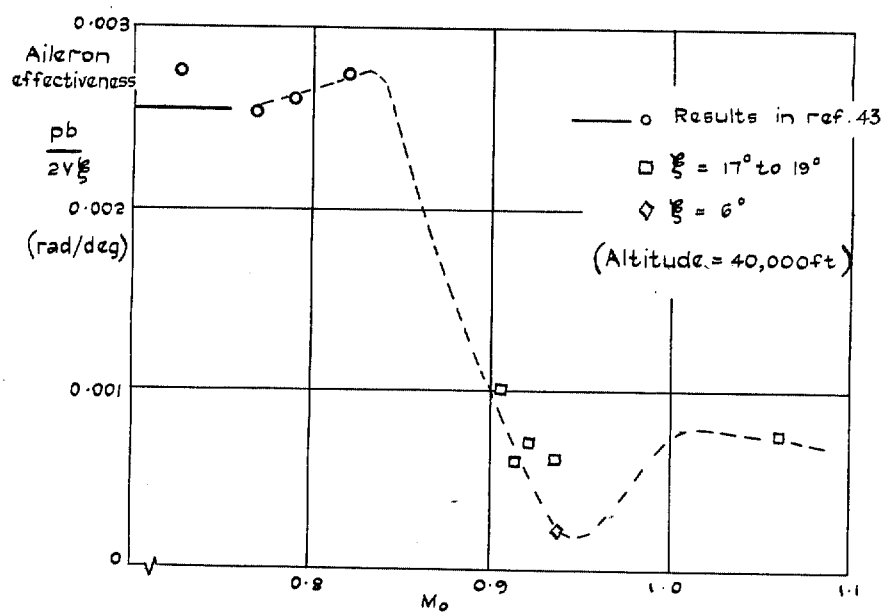

FIG. 17. Variation of aileron effectiveness with Mach number for the X–1–2 aircraft (Ref. 14).

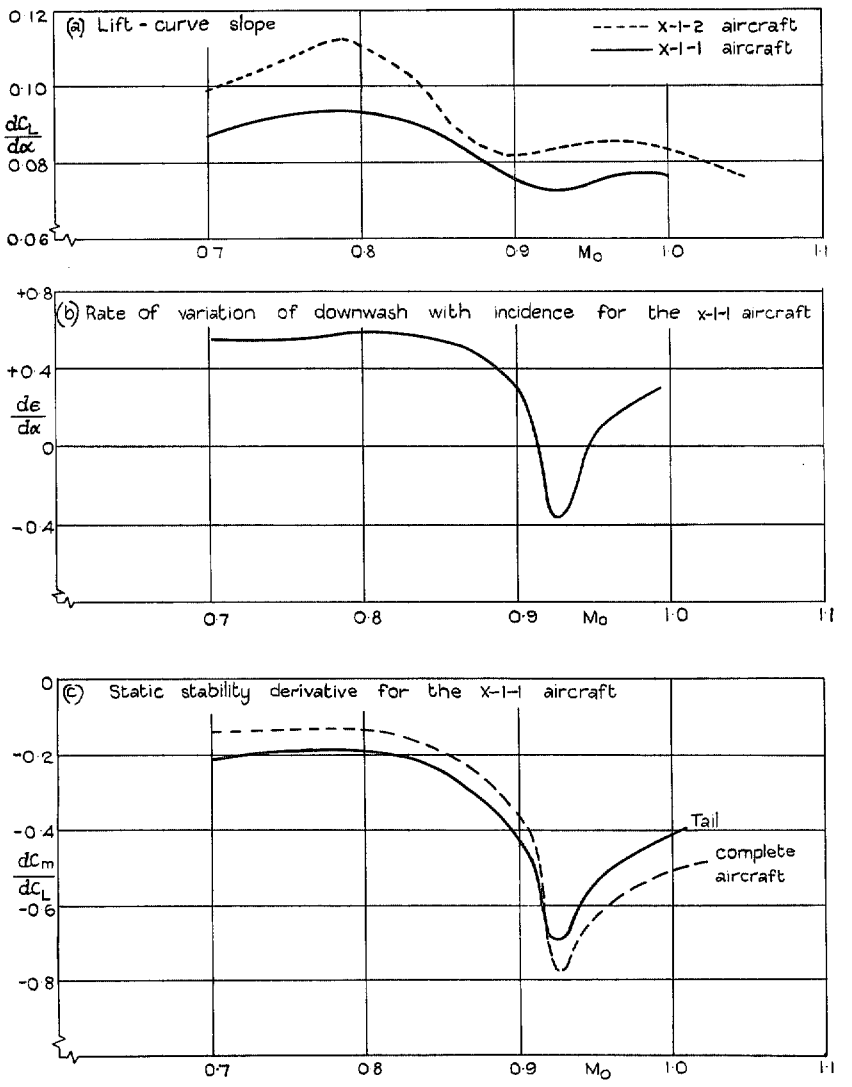

FIG. 18. Some longitudinal stability data for the X–1–1 and X–1–2 aircraft (Ref. 18).

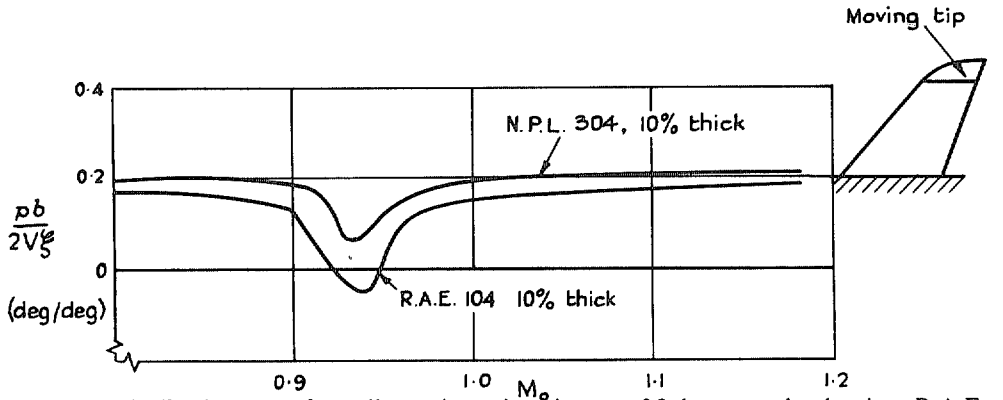

FIG. 19. Control effectiveness of an all-moving wing tip on a 35 deg sweptback wing. R.A.E. ground-launched rocket tests (Ref. 16).

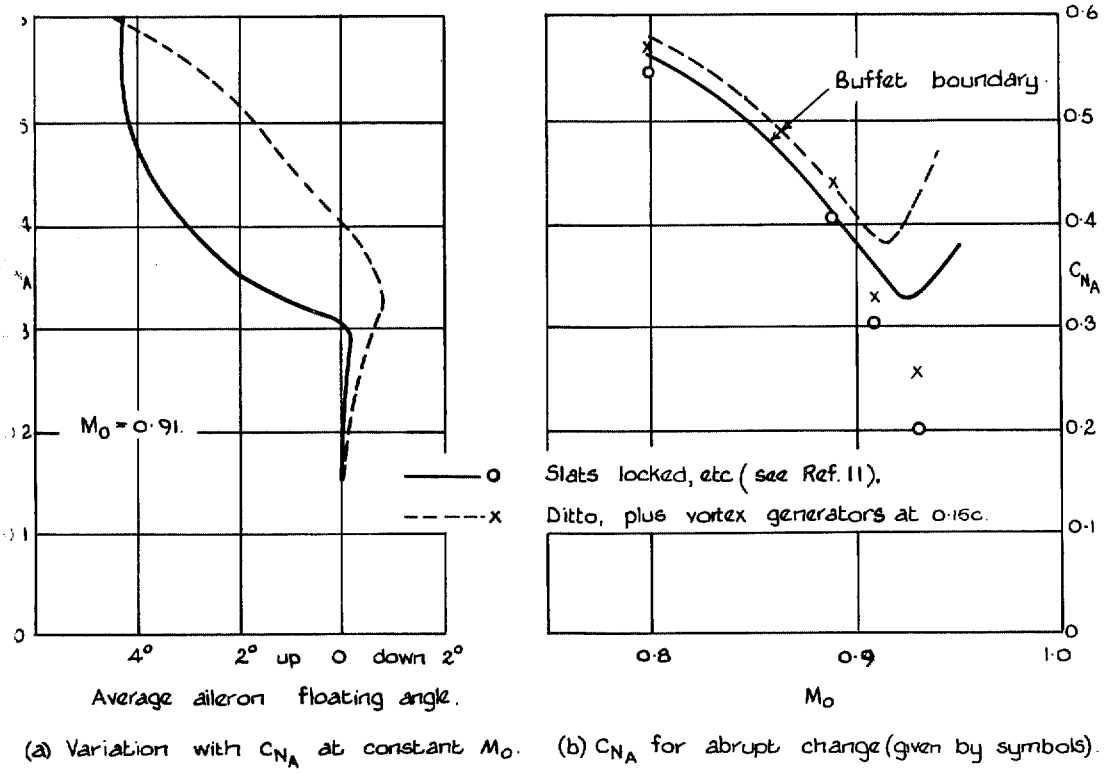

FIG. 20. Aileron floating angle on the North American F–86A–5 (Sabre) aircraft (Ref. 11).

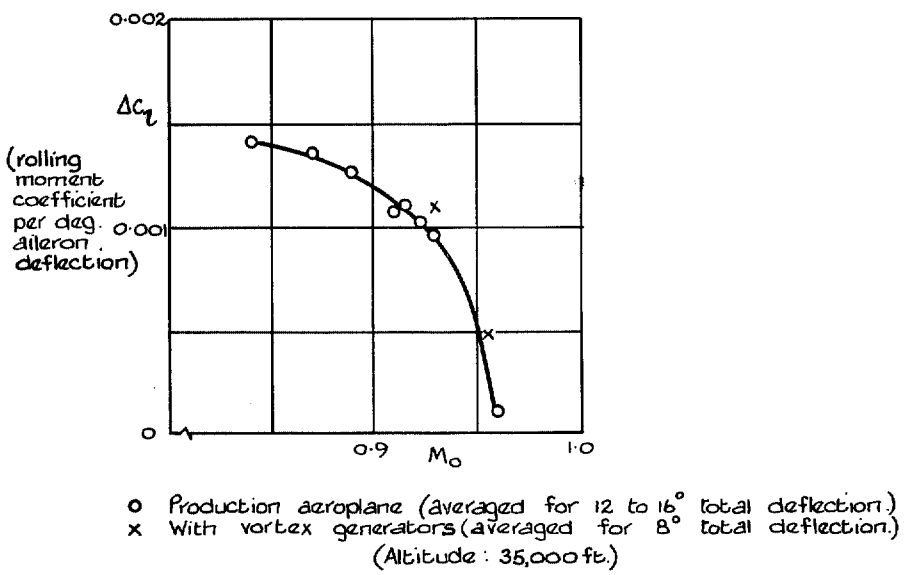

FIG. 21. Variation with Mach number of aileron rolling effectiveness F–86A–5 (Sabre) aircraft (Ref. 11).

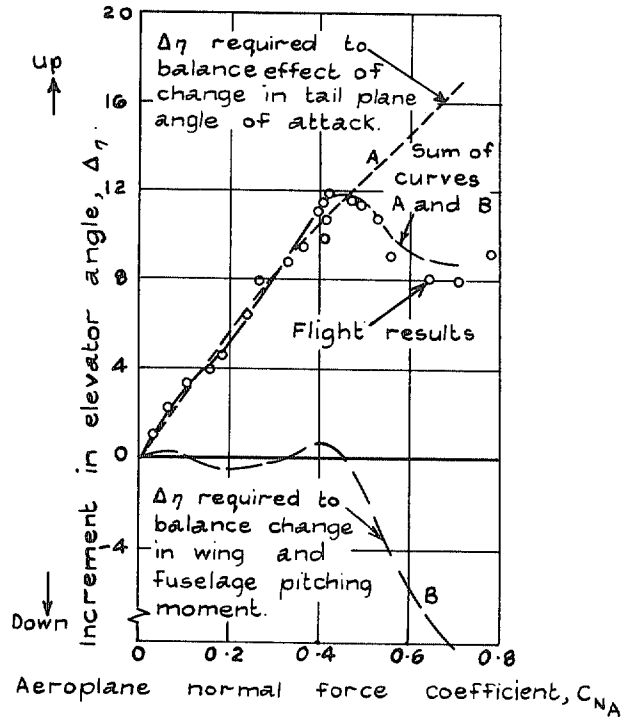

FIG. 22. Variation with C_{N_A} of elevator angle required for balance, $M_0 = 0{\cdot}87$ F86A (Sabre aircraft, Ref. 19).

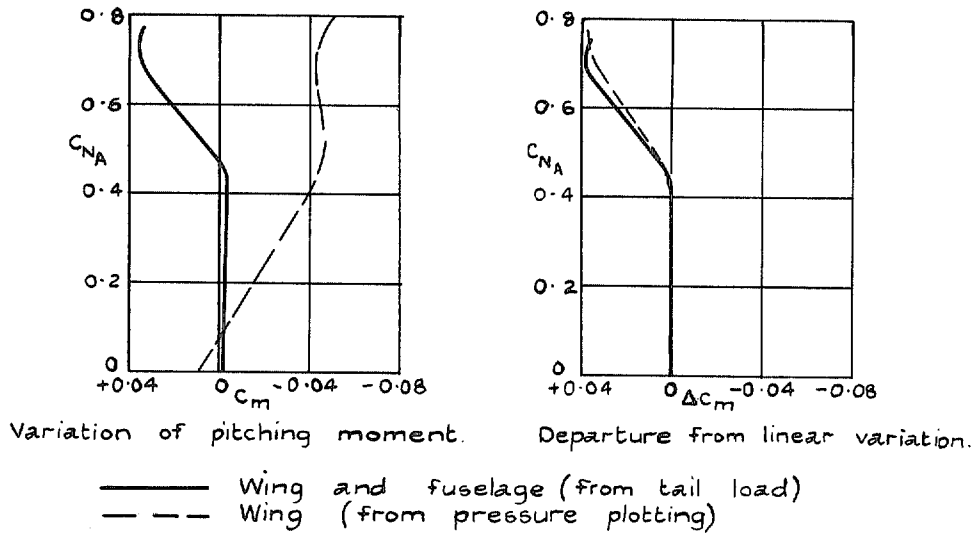

FIG. 23. Variation of C_m with C_{N_A}, as obtained from tail load measurements and panel load (pressure plotting) measurements; F86A (Sabre) (Ref. 19).

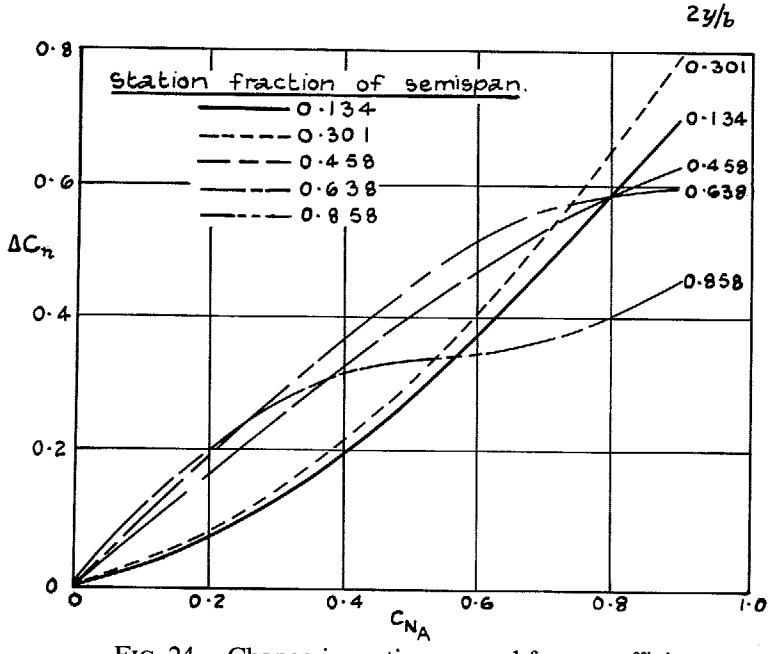

FIG. 24. Change in section normal-force coefficient with aircraft normal-force coefficient for various spanwise stations. F86A (Sabre) aircraft (Ref. 19).

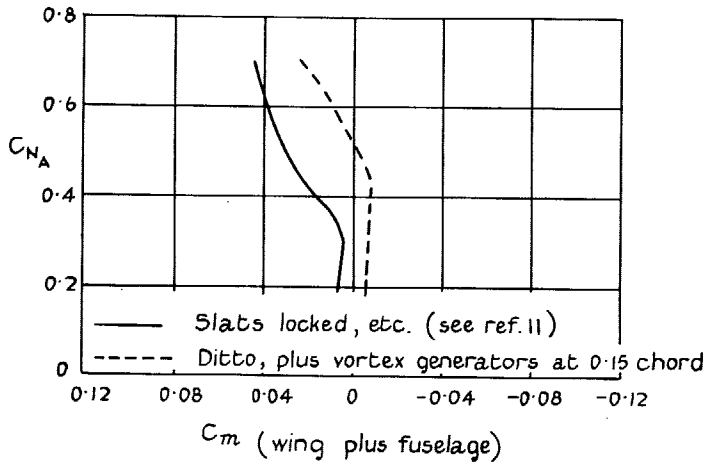

(a) Variation of C_m with C_{N_A} for $M_0 = 0.91$

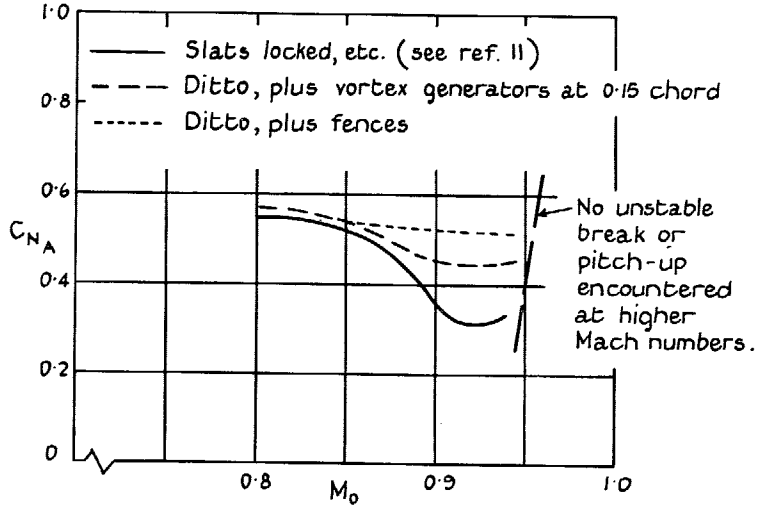

(b) Variation with M_0 of C_{N_A} for unstable break

FIG. 25a & b. The effects of vortex generators and fences on the pitch-up changes in stability for the F–86A (Sabre) aircraft (Ref. 11).

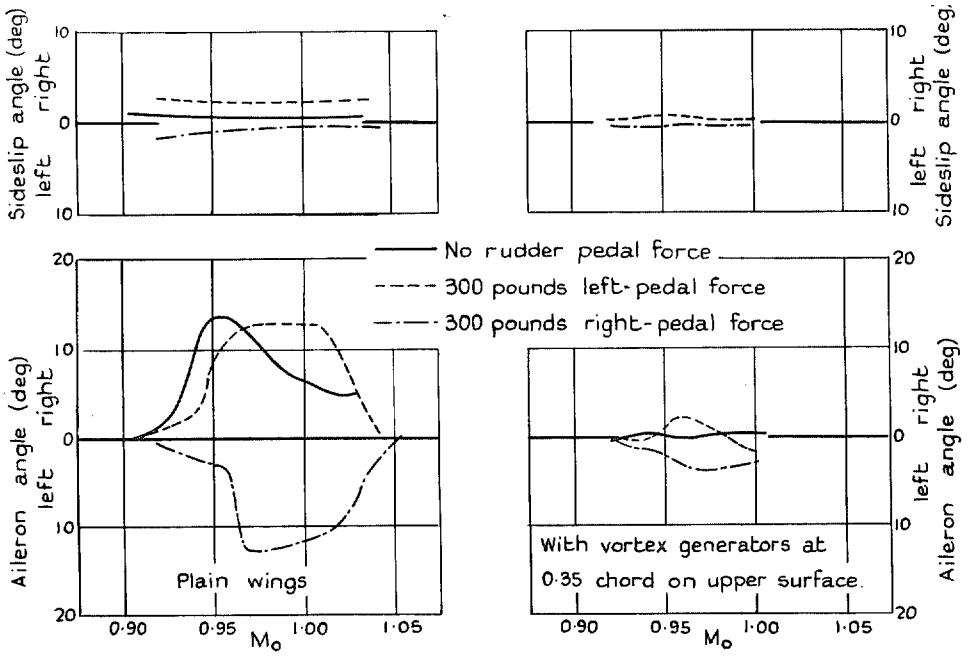

FIG. 26. 'Wing-dropping' tendency on the F–86A (Sabre) aircraft; variation of aileron angle to maintain lateral balance for different conditions of sideslip. (35,000 ft) (Ref. 11).

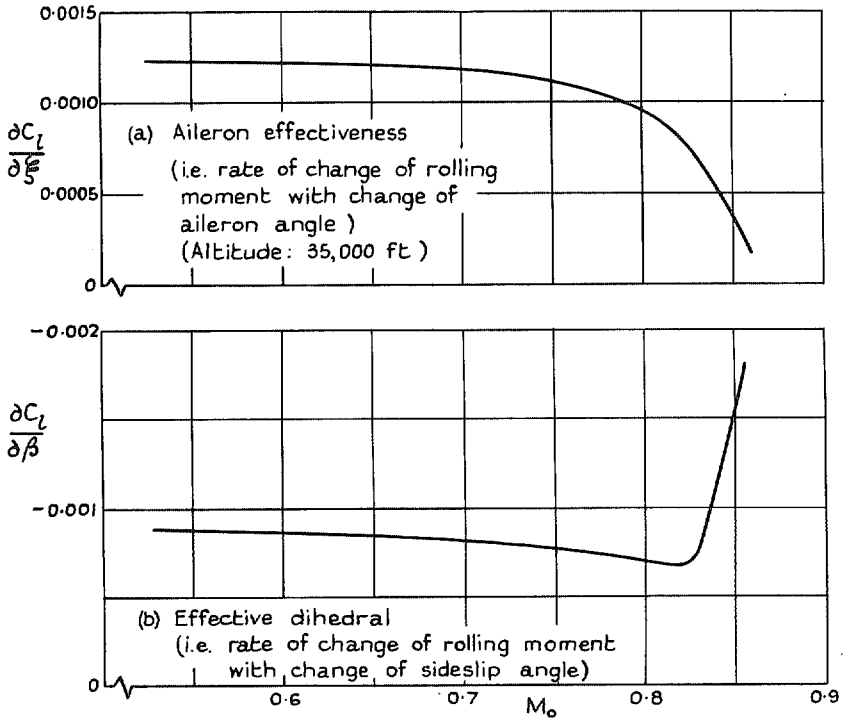

FIG. 27. Factors affecting the lateral control of a straight-wing jet aircraft which exhibited a 'wing-dropping' tendency (Ref. 23).

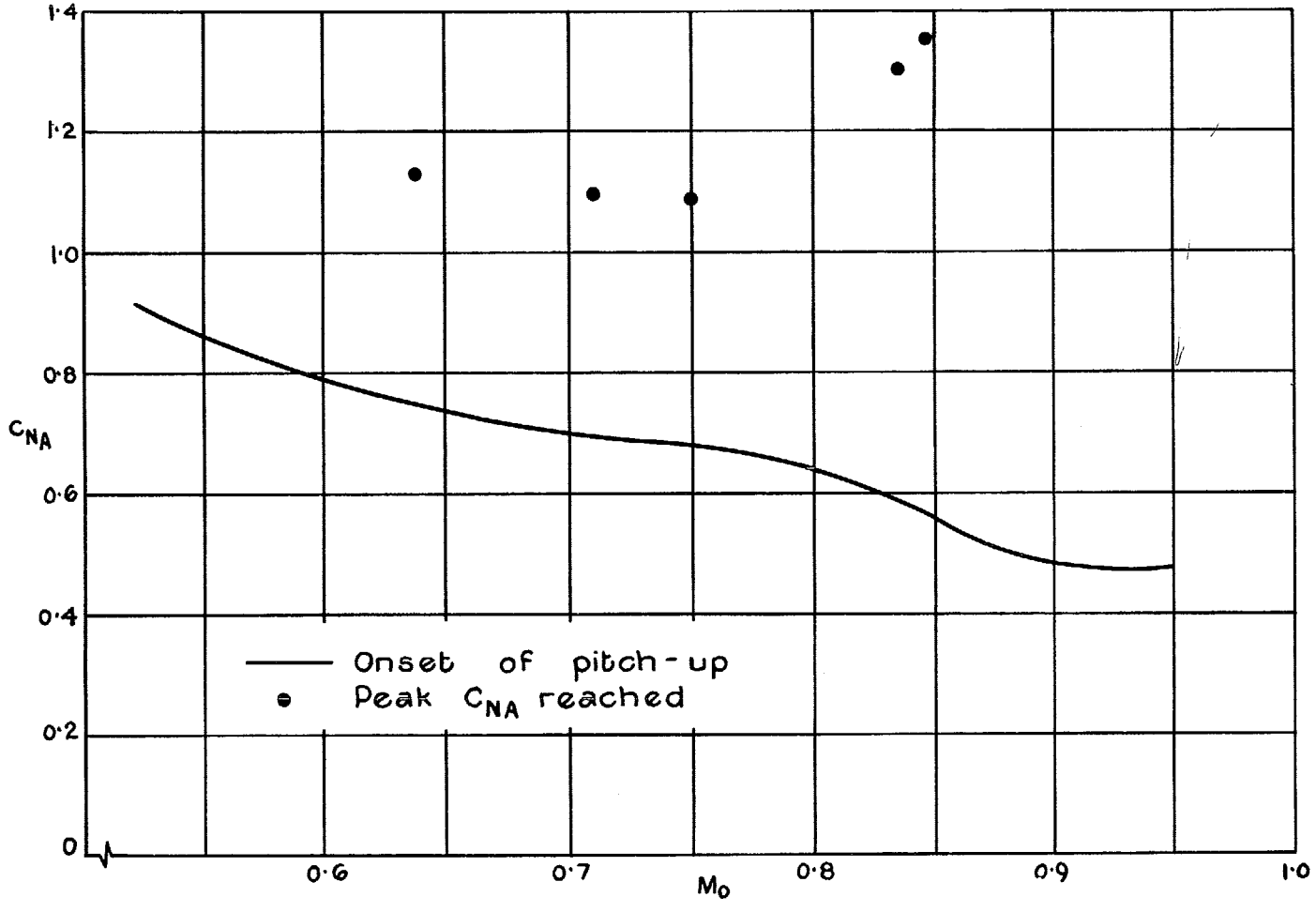

FIG. 28. Normal-force coefficient for pitch-up instability on the D–558 II aircraft (Ref. 21).

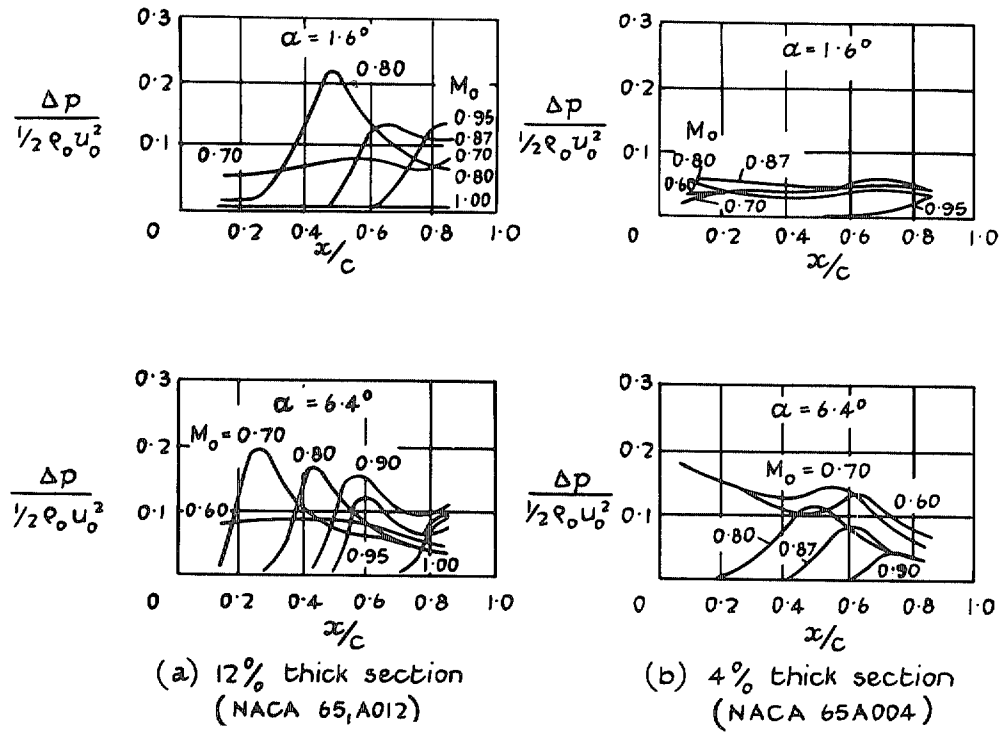

FIG. 29. Pressure fluctuations at the surfaces of two symmetrical two-dimensional aerofoils (from Ref. 26).

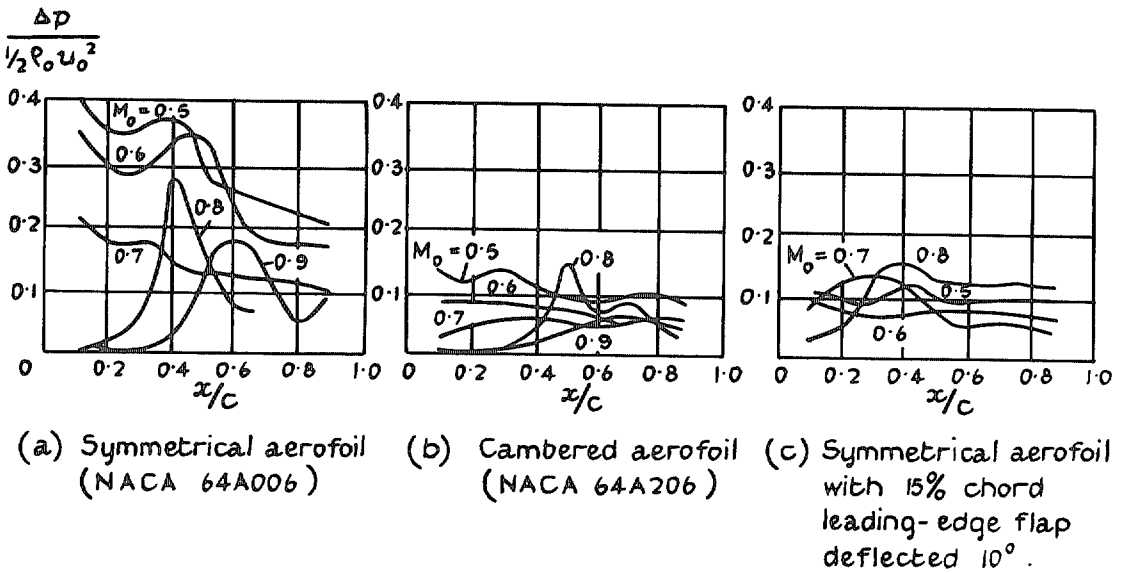

FIG. 30. The effects of camber and a leading-edge flap on the pressure fluctuations at the surface of a 6 per cent thick two-dimensional aerofoil at a normal-force coefficient $C_n = 0{\cdot}75$ (from Ref. 27).

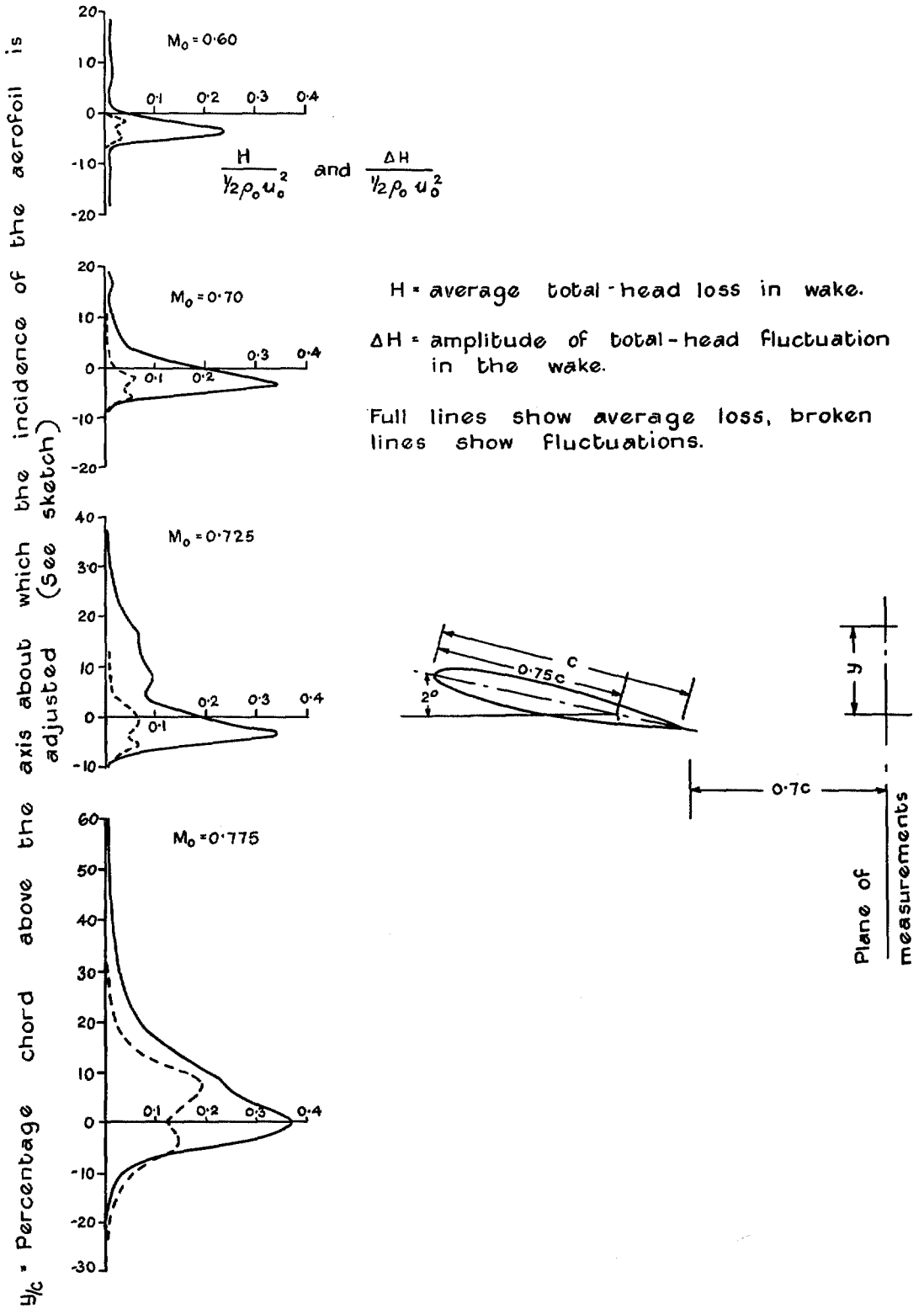

FIG. 31. Total-head fluctuations in the wake of a two-dimensional NACA 23013 aerofoil at 0·7 chord behind the trailing edge, $\alpha = 2$ deg (from Ref. 28).

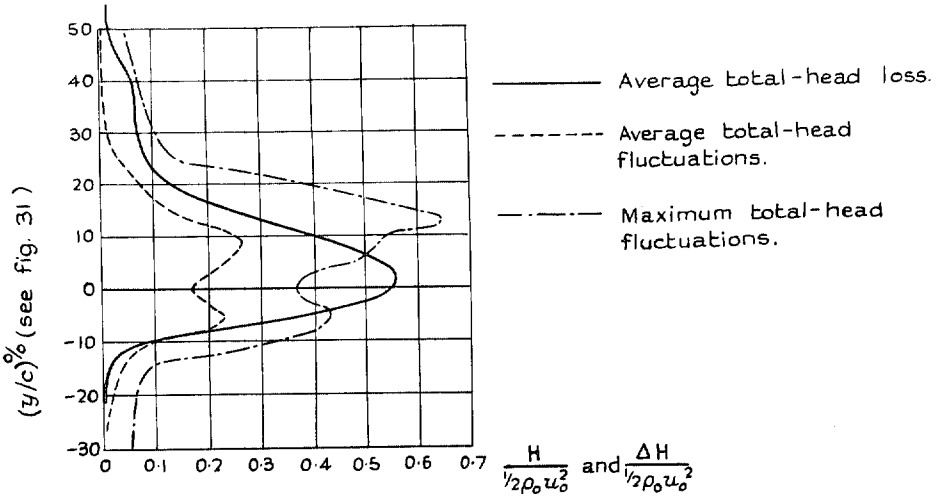

FIG. 32. Comparison between the average total-head loss, and the average and maximum total-head fluctuations at 0·7 chord behind the NACA 23013 aerofoil at $\alpha = 5$ deg, $M = 0{\cdot}75$ (from Ref. 28).

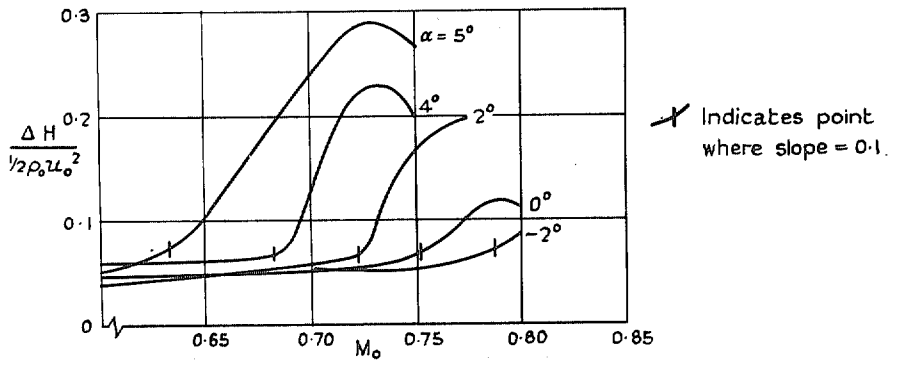

FIG. 33. Variation of maximum average total-head fluctuations with incidence and Mach number (from Ref. 28).

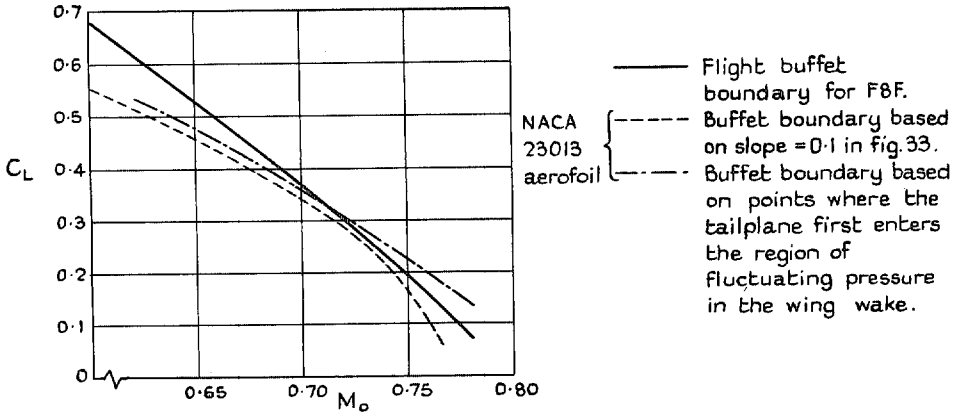

FIG. 34. Buffet boundaries estimated from the wake fluctuations, and observed in flight (from Ref. 28).

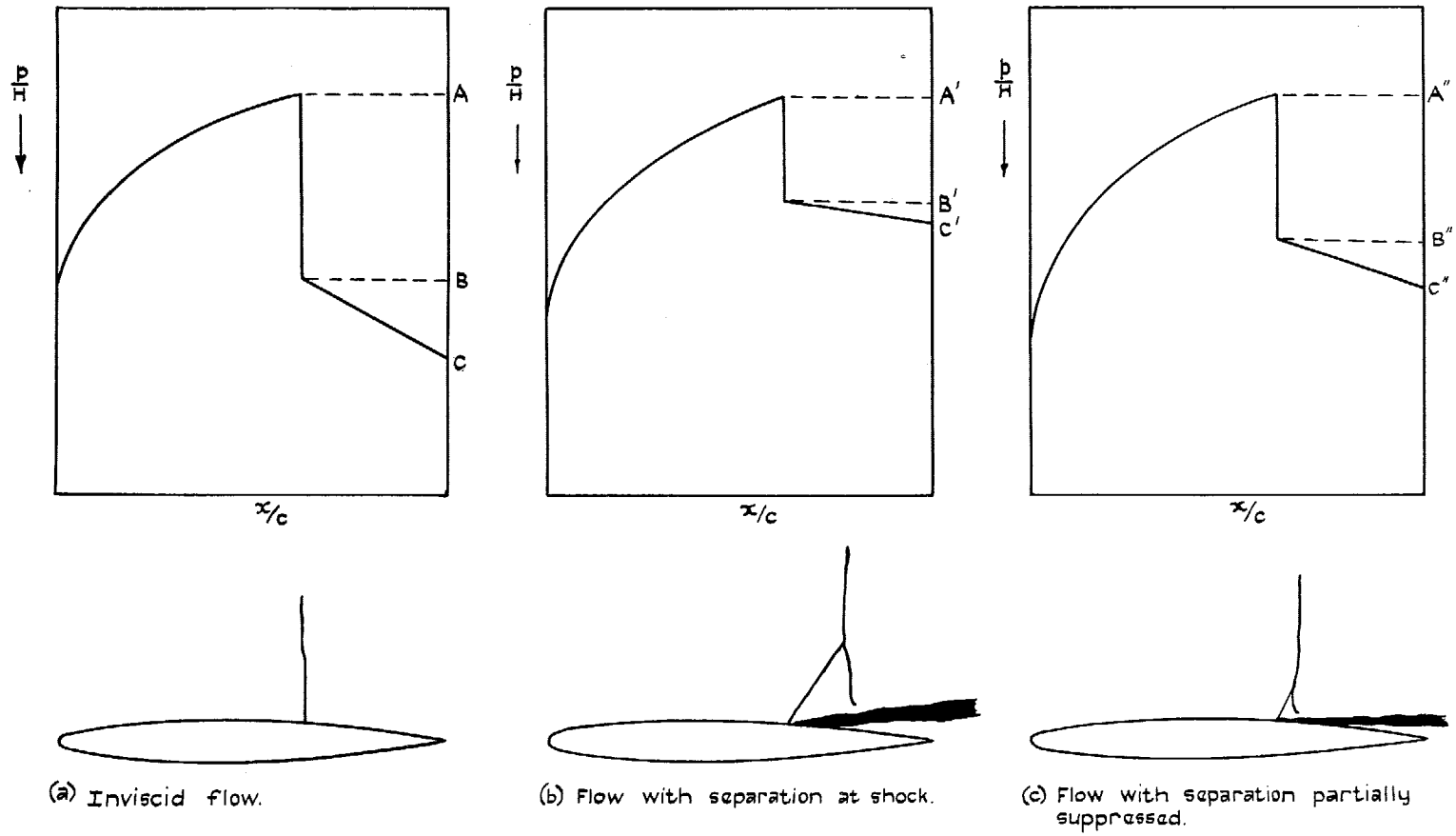

FIG. 35. The effects of shock-induced separation on the pressure recovery over the rear of an aerofoil. (Diagrammatic).

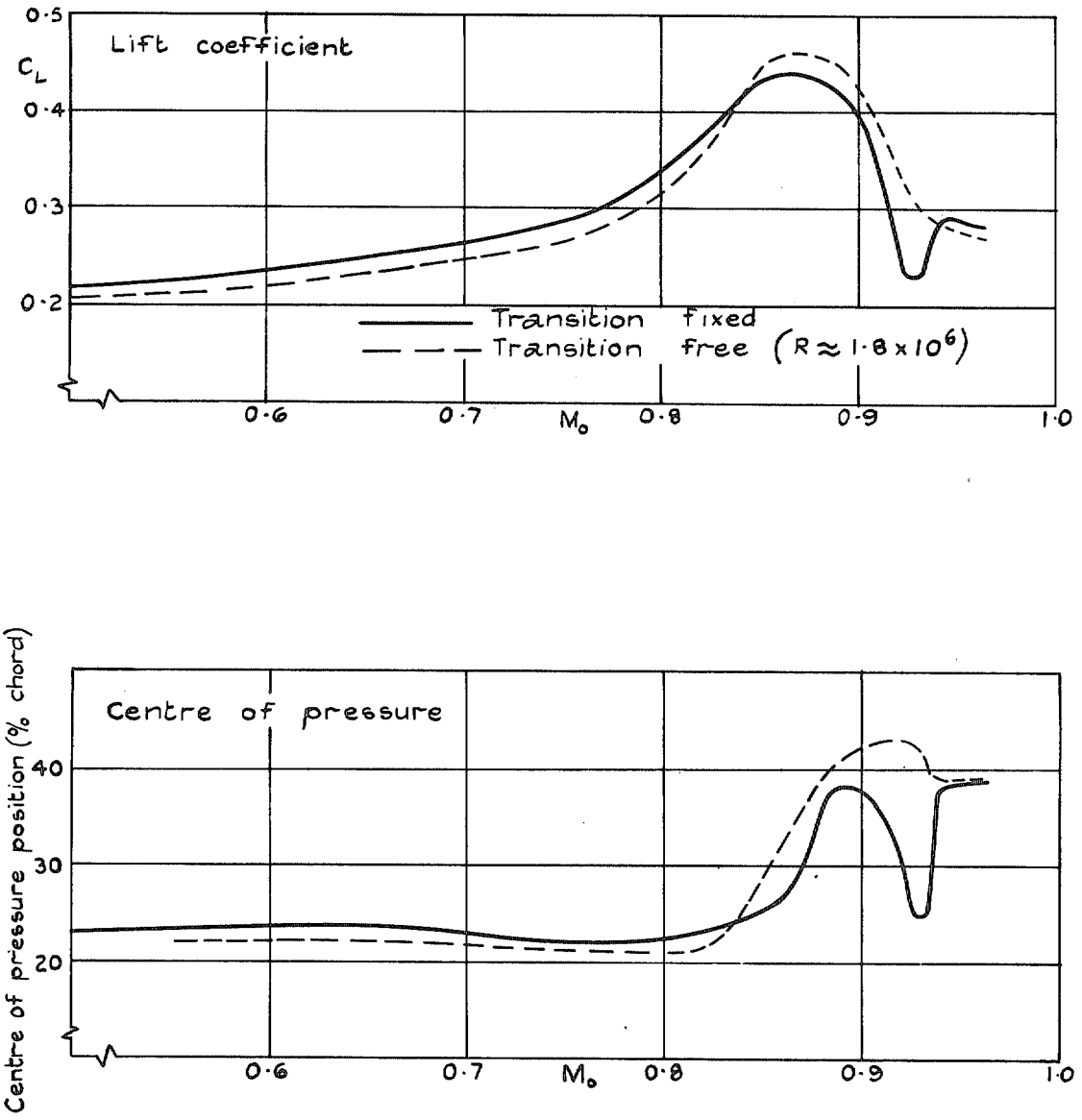

FIG. 36. Variation of lift coefficient and centre of pressure for a two-dimensional 6 per cent thick R.A.E. 104 aerofoil at 2 deg incidence (N.P.L. tunnel tests). (Results uncorrected for tunnel interference).

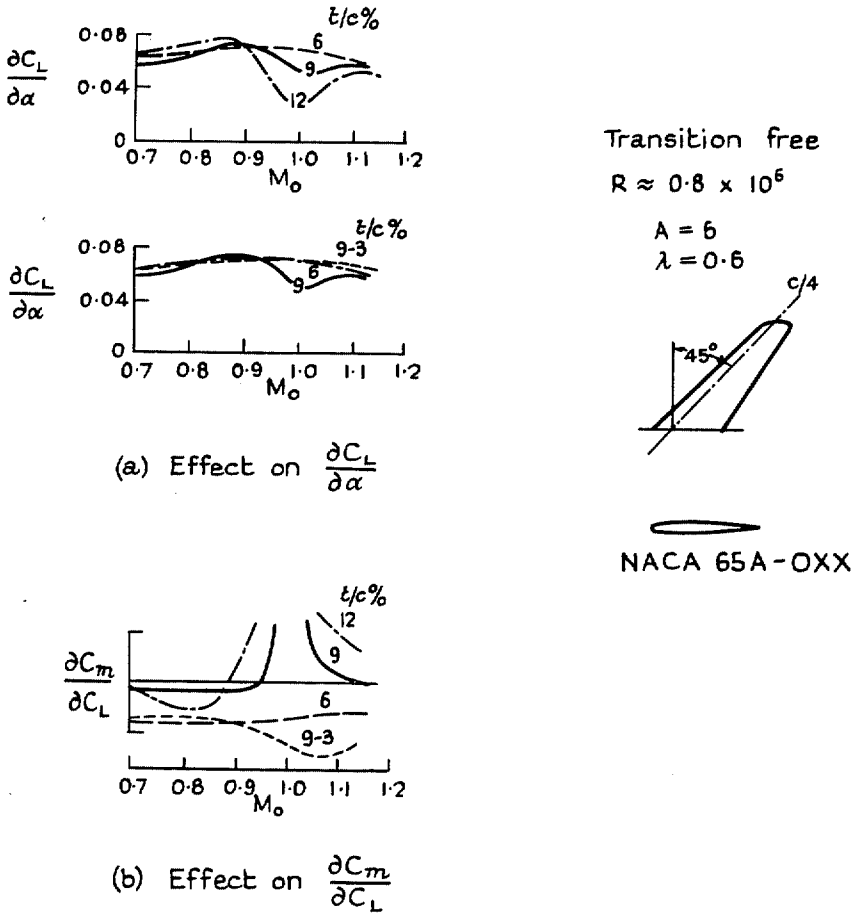

FIG. 37. Effects of section thickness for a sweptback wing (Ref. 31).

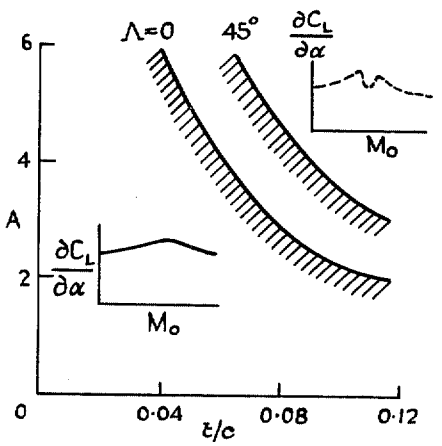

FIG. 38. Influence of aspect ratio, thickness and sweepback on the type of transonic variation of $\frac{\partial C_L}{\partial \alpha}$ (Ref. 31) transition free, low R.

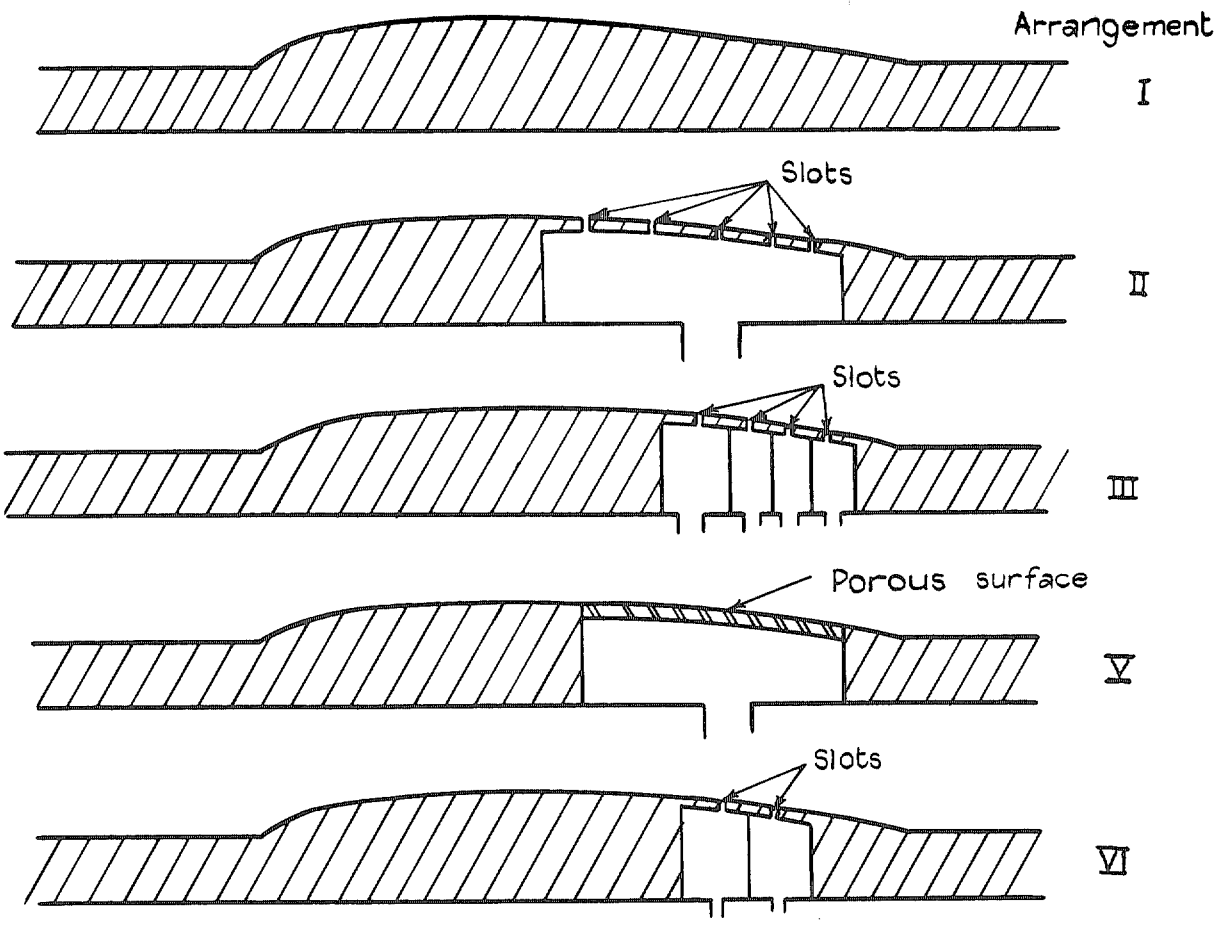

FIG. 39. Suction arrangement used in the experiment described in Ref. 33 and appropriate to Fig. 40.

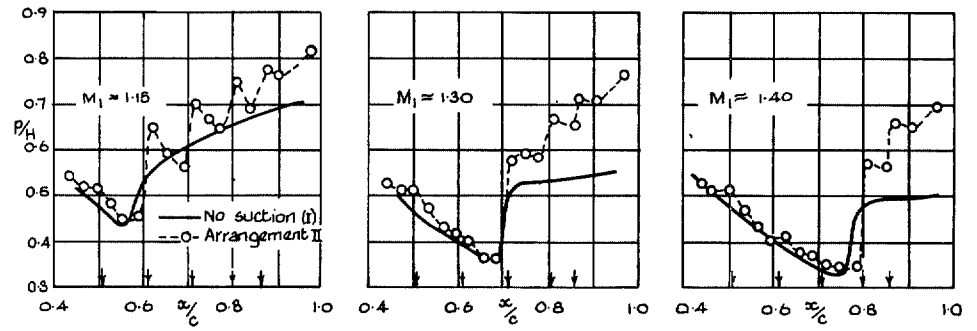

(a) Comparison of results for no suction and for slot arrangement II, for various values of M_1.

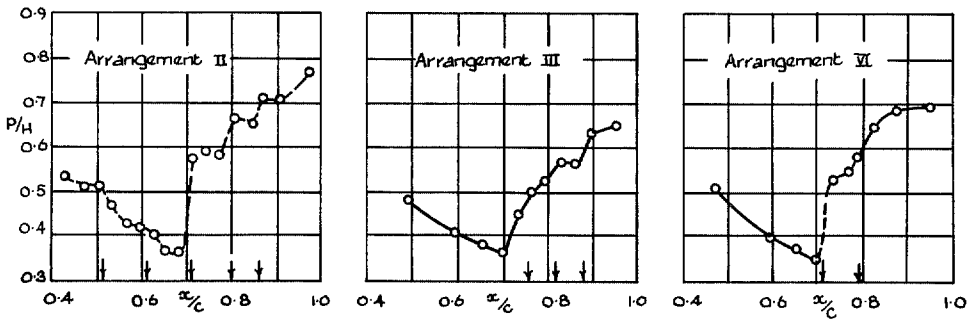

(b) Comparison of results for three arrangements of slots, $M_1 \approx 1{\cdot}30$

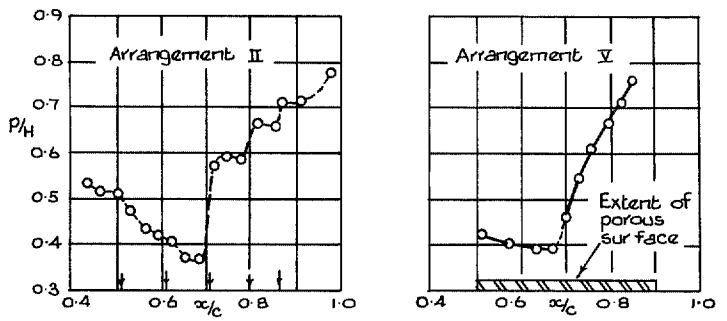

(c) Comparison of results for slot arrangement II and for porous surface, $M_1 \approx 1{\cdot}30$.

FIGS 40a to c. The effect of boundary-layer suction on the pressure recovery at and downstream of a shock wave on the curved wall of a nozzle (*see* Fig. 39) (Ref. 33).
(Arrows represent the location of the slots in use).

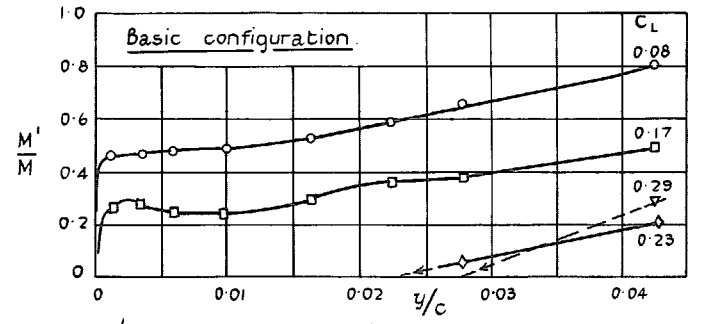

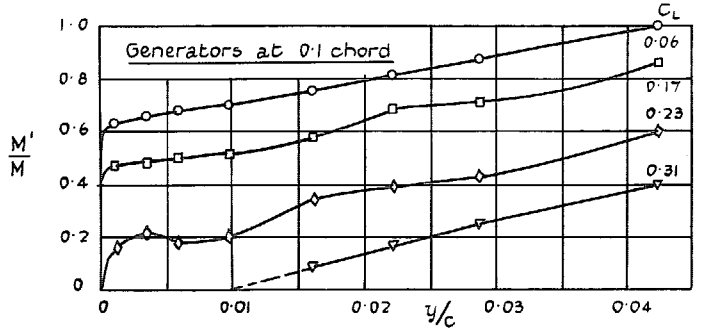

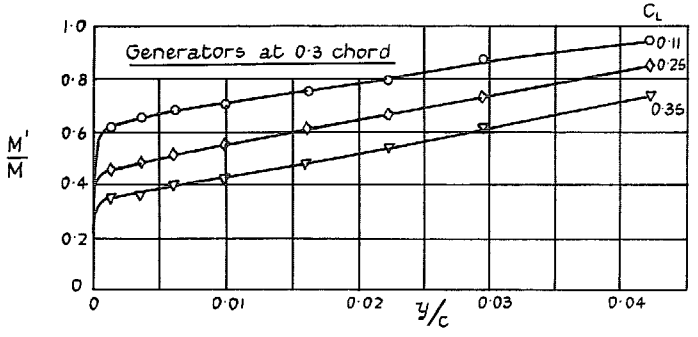

FIG. 41. Boundary-layer traverses at the trailing edge of the F–51D aircraft; effect of a single row of counter-rotating vortex generators; $M_0 = 0{\cdot}745$ (Ref. 35).

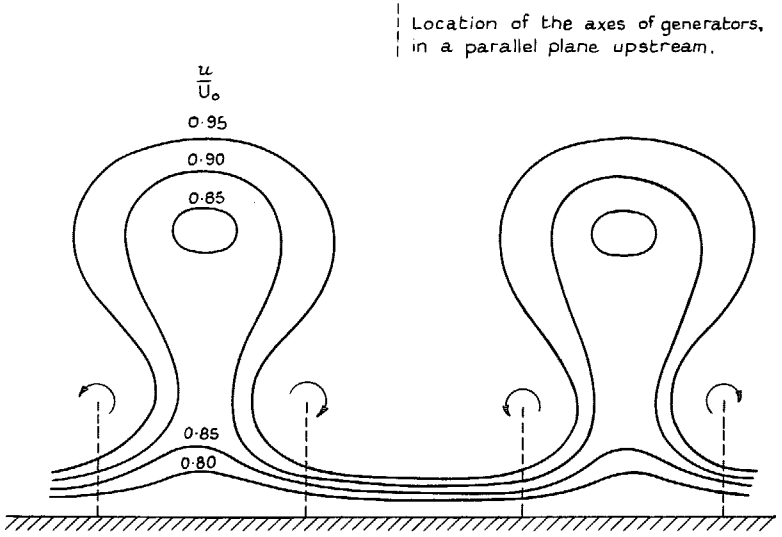

FIG. 42. Sketch of velocity contours in a plane normal to the main stream direction (into paper) at about 15 generator heights downstream of vortex generators (shown here counter rotating).

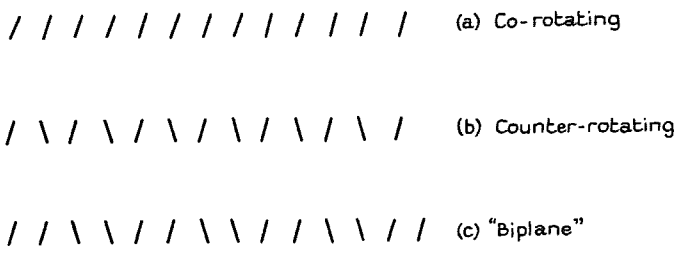

FIG. 43. Plan views of alternative arrangements of vortex generators.

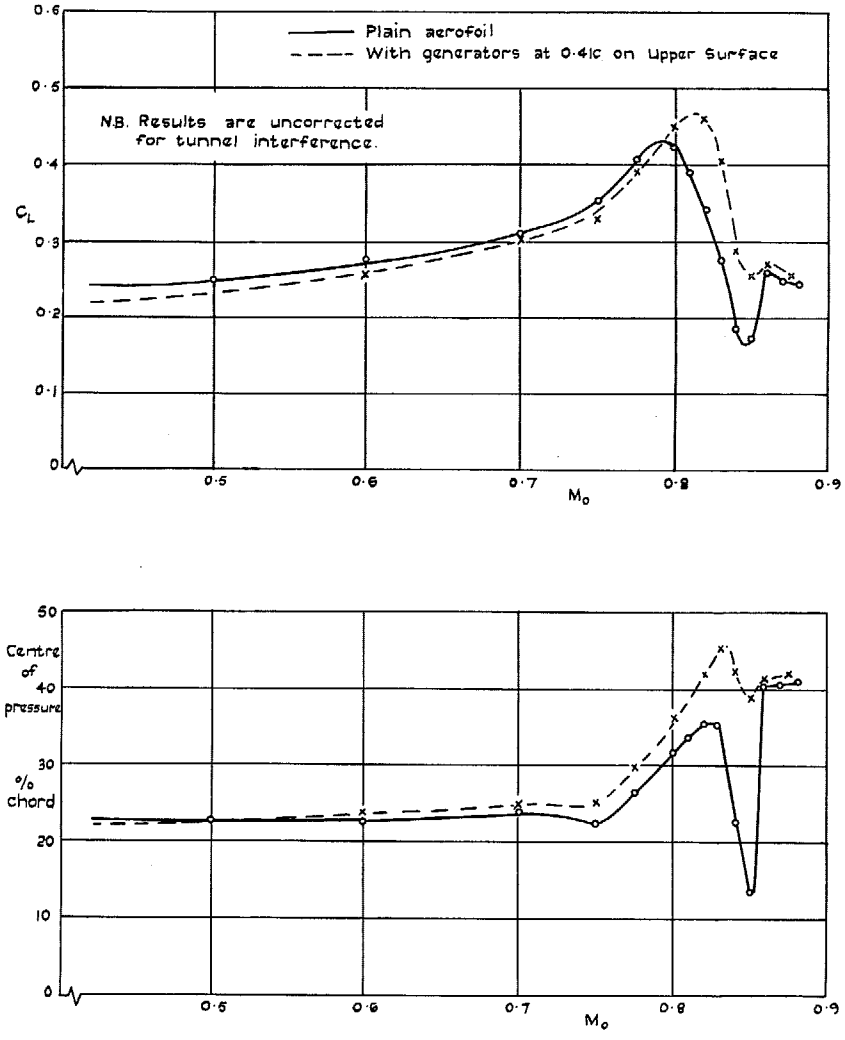

FIG. 44. The effects of vortex generators on a 10 per cent thick R.A.E. 102 section at $\alpha = 2$ deg; lift and centre of pressure.

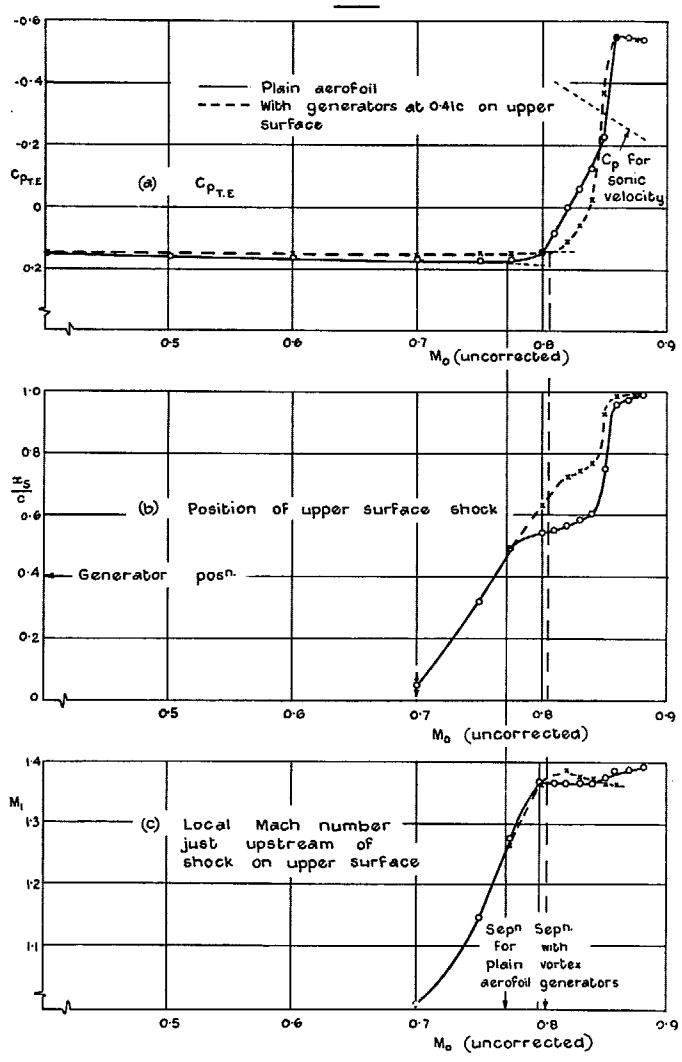

FIG. 45. The effects of vortex generators on a 10 per cent thick R.A.E. 102 section at $\alpha = 2$ deg; $C_{pT.E.}$, position of upper surface shock, and M_1.

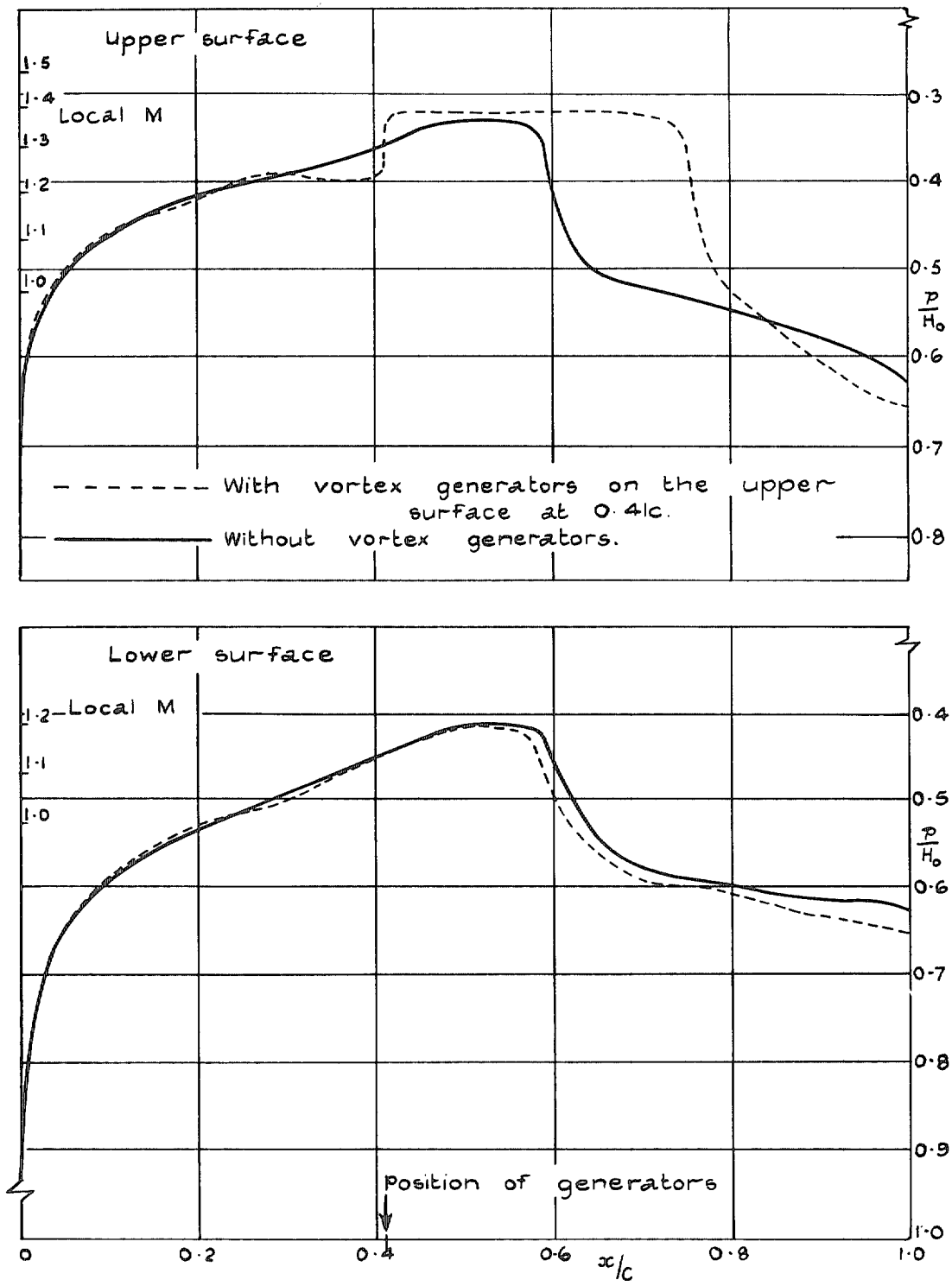

FIG. 46. The effects of vortex generators on a 10 per cent thick R.A.E. 102 section at $\alpha = 2$ deg; pressure distributions at $M_0 = 0{\cdot}83$ (uncorrected).

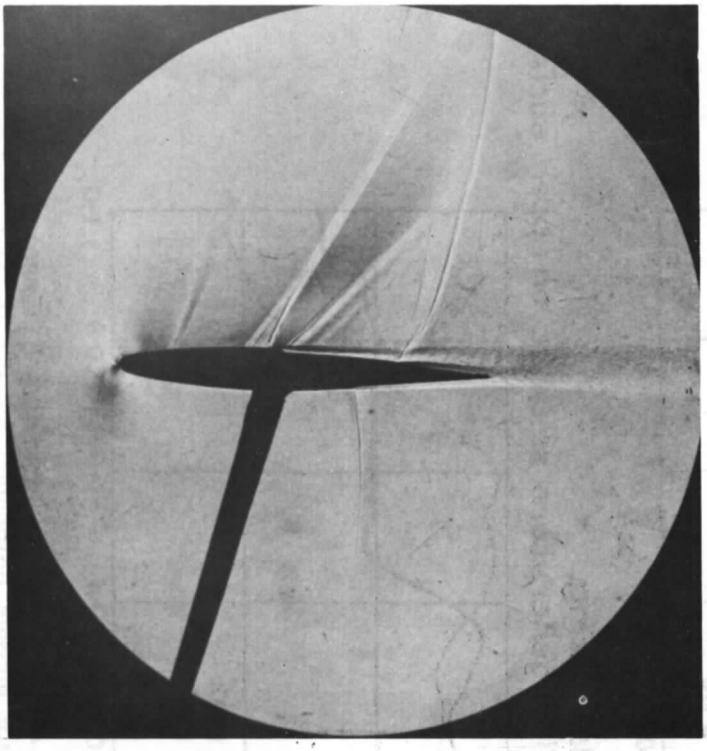

FIG. 47. Effect of vortex generators on shock induced separation of a turbulent boundary layer. 10 per cent thick R.A.E. 102 at 2 deg incidence.

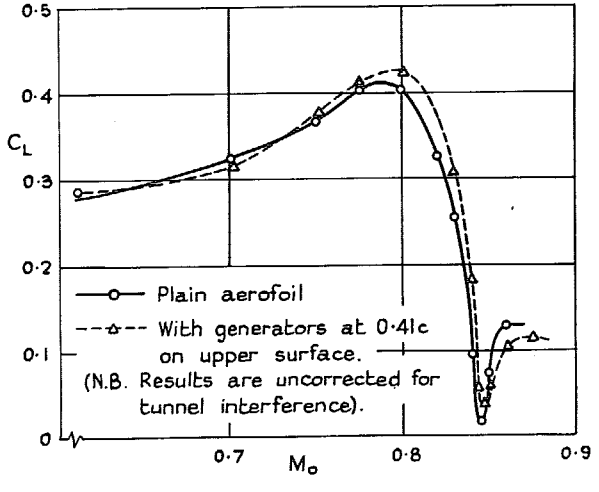

FIG. 48. The effects of vortex generators on the lift due to a 0·25c plain flap ($\xi = 4$ deg) on a 10 per cent thick R.A.E. 102 section ($\alpha = 0$ deg).

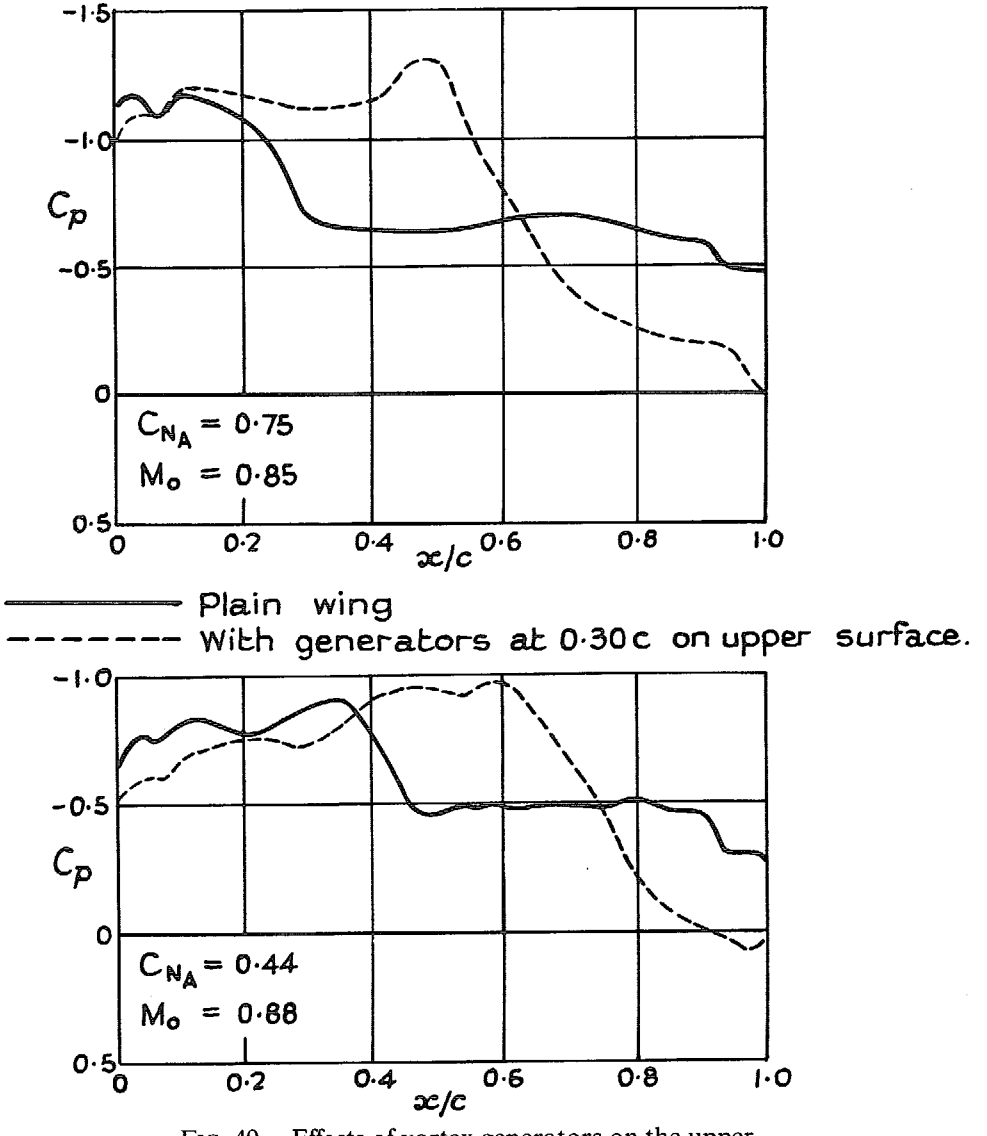

FIG. 49. Effects of vortex generators on the upper surface pressure distribution for the D–558–I aircraft (Ref. 36).

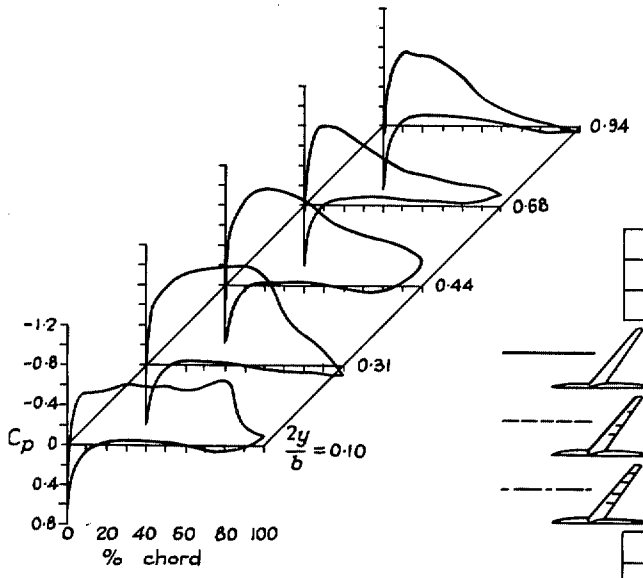

Chordwise pressure distributions without fences.

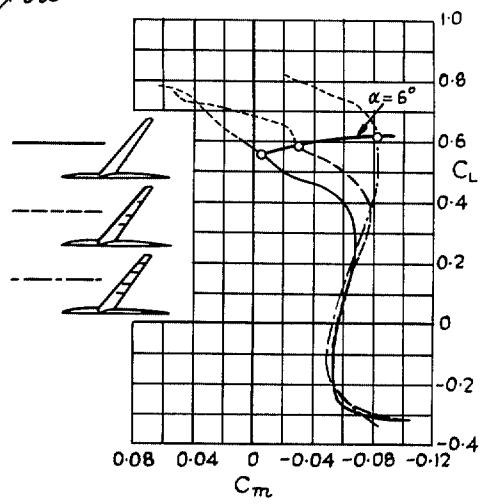

Variation of pitching moment with C_L for wing and fuselage.

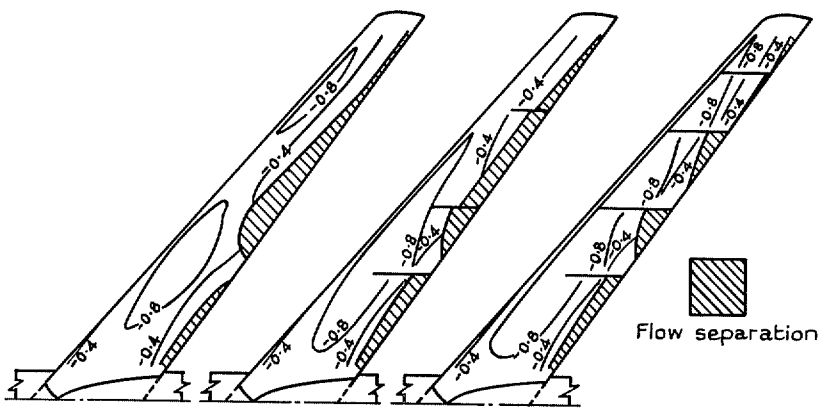

Approximate regions of separated flow (and lines of constant C_p) without and with fences. $\alpha = 6°$.

FIG. 50. Effects of fences on a cambered and twisted sweptback wing (Ref. 42). $M_0 = 0{\cdot}9$, $R = 2 \times 10^6$, transition free.

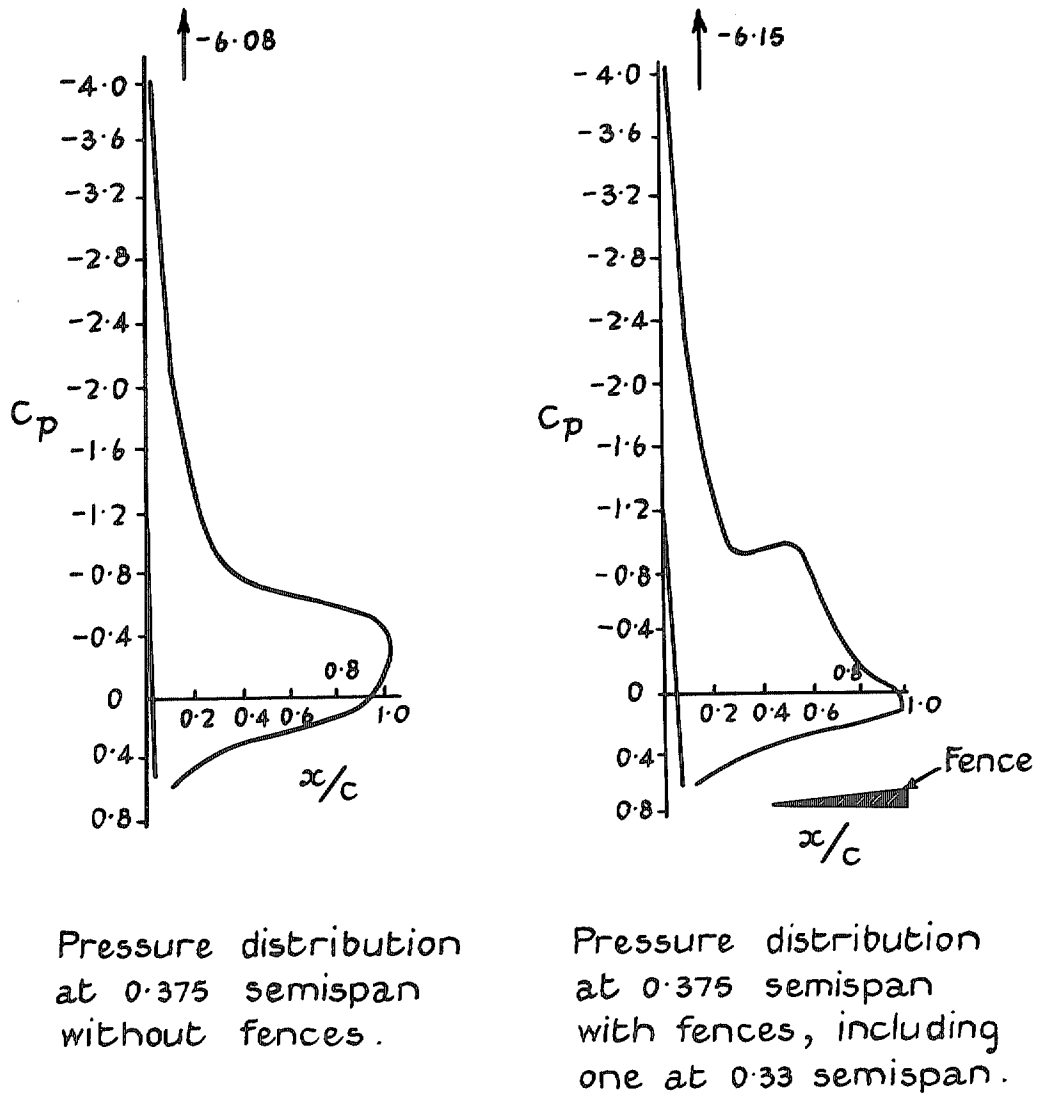

FIG. 51. Effect of fences on a sweptback wing at low speeds (Wing shape shown in fig. 50) (Ref. 42). $M_0 = 0{\cdot}25$, $R = 2 \times 10^6$.

Printed in Wales for Her Majesty's Stationery Office
by Allen Printers (Wales) Limited

Dd.129527 K5

Published by
HER MAJESTY'S STATIONERY OFFICE

To be purchased from
49 High Holborn, London W.C.1
423 Oxford Street, London W.1
13A Castle Street, Edinburgh 2
109 St. Mary Street, Cardiff CF1 1JW
Brazennose Street, Manchester 2
50 Fairfax Street, Bristol 1
258–259 Broad Street, Birmingham 1
7–11 Linenhall Street, Belfast BT2 8AY
or through any bookseller

S.O. Code No. 23–3510